AFRL-RX-WP-TR-2009-4330

ACCELERATED INSERTION OF MATERIALS-ELECTRONICS (AIM-E)

Delivery Order 0011: Production of Electronic Type-Specific Buckytubes for Next Generation Defense Electronics

Christina Chen

University of Dayton Research Institute

OCTOBER 2009
Final Report

AIR FORCE RESEARCH LABORATORY
MATERIALS AND MANUFACTURING DIRECTORATE
WRIGHT-PATTERSON AIR FORCE BASE, OH 45433-7750
AIR FORCE MATERIEL COMMAND
UNITED STATES AIR FORCE

NOTICE AND SIGNATURE PAGE

Using Government drawings, specifications, or other data included in this document for any purpose other than Government procurement does not in any way obligate the U.S. Government. The fact that the Government formulated or supplied the drawings, specifications, or other data does not license the holder or any other person or corporation; or convey any rights or permission to manufacture, use, or sell any patented invention that may relate to them.

This report is the result of contracted fundamental research deemed exempt from public affairs security and policy review in accordance with SAF/AQR memorandum dated 10 Dec 08 and AFRL/CA policy clarification memorandum dated 16 Jan 09. This report is available to the general public, including foreign nationals. Copies may be obtained from the Defense Technical Information Center (DTIC) (http://www.dtic.mil).

AFRL-RX-WP-TR-2009-4330 HAS BEEN REVIEWED AND IS APPROVED FOR PUBLICATION IN ACCORDANCE WITH ASSIGNED DISTRIBUTION STATEMENT.

*//Signature//

JOHN BOECKL
AFRL/RXPS Work Unit Manager

//Signature//

JOSEPH A. BAKER
AFRL/RXPS Branch Chief

//Signature//

KAREN OLSON
AFRL/RXPS Deputy Division Chief, Acting

This report is published in the interest of scientific and technical information exchange, and its publication does not constitute the Government's approval or disapproval of its ideas or findings.

*Disseminated copies will show "//Signature//" stamped or typed above the signature blocks.

REPORT DOCUMENTATION PAGE

Form Approved
OMB No. 0704-0188

1. REPORT DATE *(DD-MM-YY)*	2. REPORT TYPE	3. DATES COVERED *(From - To)*
October 2009	Final	13 March 2008 - 16 September 2009

4. TITLE AND SUBTITLE
ACCELERATED INSERTION OF MATERIALS-ELECTRONICS (AIM-E) Delivery Order 0011: Production of Electronic Type-Specific Buckytubes for Next Generation Defense Electronics

5a. CONTRACT NUMBER
FA8650-06-D-5401-0011

5b. GRANT NUMBER

5c. PROGRAM ELEMENT NUMBER
62102F

6. AUTHOR(S)
Christina Chen (Jordan Valley Innovation Center)

5d. PROJECT NUMBER
4348

5e. TASK NUMBER
80

5f. WORK UNIT NUMBER
PS113100

7. PERFORMING ORGANIZATION NAME(S) AND ADDRESS(ES)

University of Dayton Research Institute
300 College Park
Dayton, OH 45469-0101

Jordan Valley Innovation Center
Missouri State University
524 North Boonville Avenue
Springfield, MO 65806

8. PERFORMING ORGANIZATION REPORT NUMBER

9. SPONSORING/MONITORING AGENCY NAME(S) AND ADDRESS(ES)

Air Force Research Laboratory
Materials and Manufacturing Directorate
Wright-Patterson Air Force Base, OH 45433-7750
Air Force Materiel Command
United States Air Force

10. SPONSORING/MONITORING AGENCY ACRONYM(S)
AFRL/RXPS

11. SPONSORING/MONITORING AGENCY REPORT NUMBER(S)
AFRL-RX-WP-TR-2009-4330

12. DISTRIBUTION/AVAILABILITY STATEMENT
Approved for public release; distribution unlimited.

13. SUPPLEMENTARY NOTES
This report is the result of contracted fundamental research deemed exempt from public affairs security and policy review in accordance with SAF/AQR memorandum dated 10 Dec 08 and AFRL/CA policy clarification memorandum dated 16 Jan 09. Report contains color.

14. ABSTRACT
This effort has focused on several key issues to separating buckytubes. Initially the raw buckytube starting material was evaluated to ensure that the best possible results from the separation methods would be achieved. Once this evaluation completed, several separation methods were evaluated. The work on this separation methodology and the scale-up to larger batch processes is continuing.

15. SUBJECT TERMS

16. SECURITY CLASSIFICATION OF:			17. LIMITATION OF ABSTRACT:	18. NUMBER OF PAGES	19a. NAME OF RESPONSIBLE PERSON (Monitor)
a. REPORT	b. ABSTRACT	c. THIS PAGE			John Boeckl
Unclassified	Unclassified	Unclassified	SAR	44	19b. TELEPHONE NUMBER *(Include Area Code)* N/A

Standard Form 298 (Rev. 8-98)
Prescribed by ANSI Std. Z39-18

1.2 Table of Contents

1.3 Technical Information

1.3.1 Introduction

The Jordan Valley Innovation Center at Missouri State University (JVIC-MSU) along with Unidym, Inc. and Brewer Science, Inc. (BSI) worked to develop and scale up a supply of buckytubes having specific electrical properties. The "Production of Electronic Type-Specific Buckytubes for Next-Generation Electronics" covered three main tasks which included the production of the raw single walled carbon nanotubes (SWNTs), the refinement of the raw SWNT material to yield a high purity electronic type separated form of the original material, and finally materials electronic properties characterization and device application. The first task was performed by Unidym, Inc., the second task was performed by BSI, and the last task was performed by JVIC-MSU. The following is a summary of the task performed by each project partner and the conclusions that resulted.

1.3.2 Subcontractor: Unidym Task Summary

1.3.2.1 Buckytube Synthesis, Quality and Diameter Control

Unidym Inc.'s portion of the project was to supply regular HiPCO "as-produced" SWNT Buckytubes. Referred to as "R" grade SWNTs, during the initial screening of these materials 2 lots were provided to BSI, which were determined to have important protocols for further refinement. Initially, Unidym investigated various QC tools to study these "R" grade lots, such that they can relate the QC variables for synthesis conditions. A Thermal Gravimetric Analysis (TGA) conducted showed differences in purity levels between the 2 lots that were initially investigated. These initial TGA results show differences in both the catalyst level and the peak burn-off temperature as shown in figure 1.

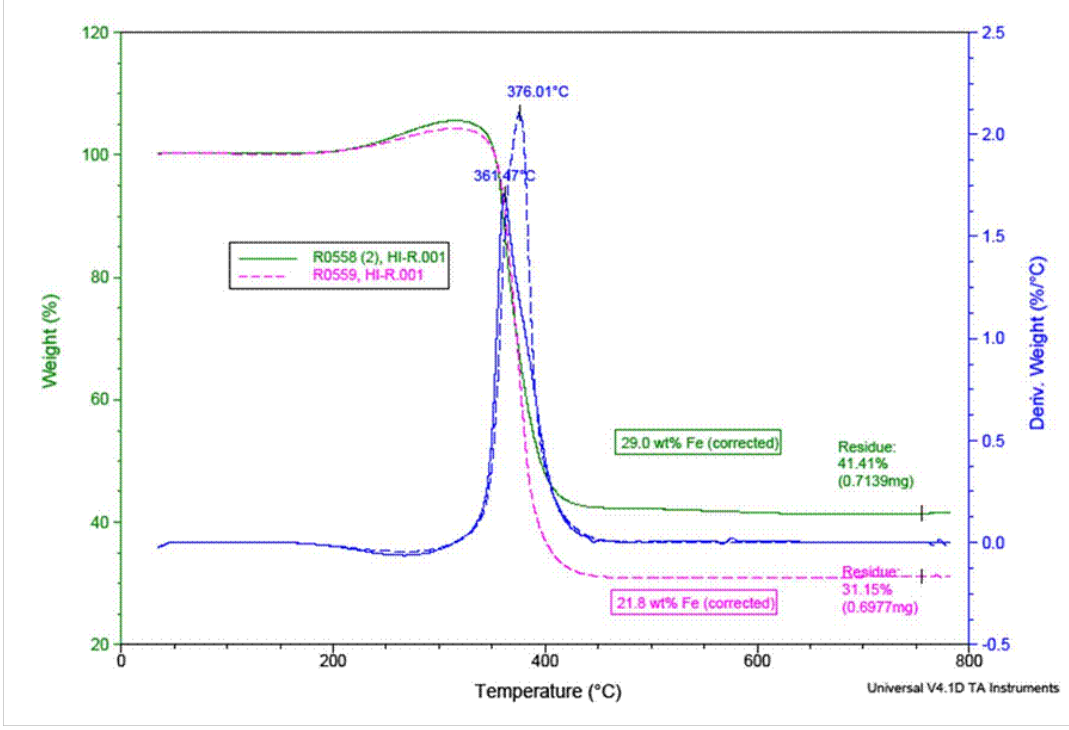

Figure 1: TGA graph of the 2 lots of HiPCO "R" Grade SWNTs

During the period of performance of this project, a number of batches (12) were provided to BSI for further refinement. Unidym was also developing an alternative method of SWNT production,

specifically, an MGPx process with emphasis on diameter and chirality control. Initial results were encouraging, with SWNTs being produced with diameters comparable to HiPCO material (figure 2). As the project progressed, different batches of the two buckytube synthesis techniques were produced for further analysis and refinement.

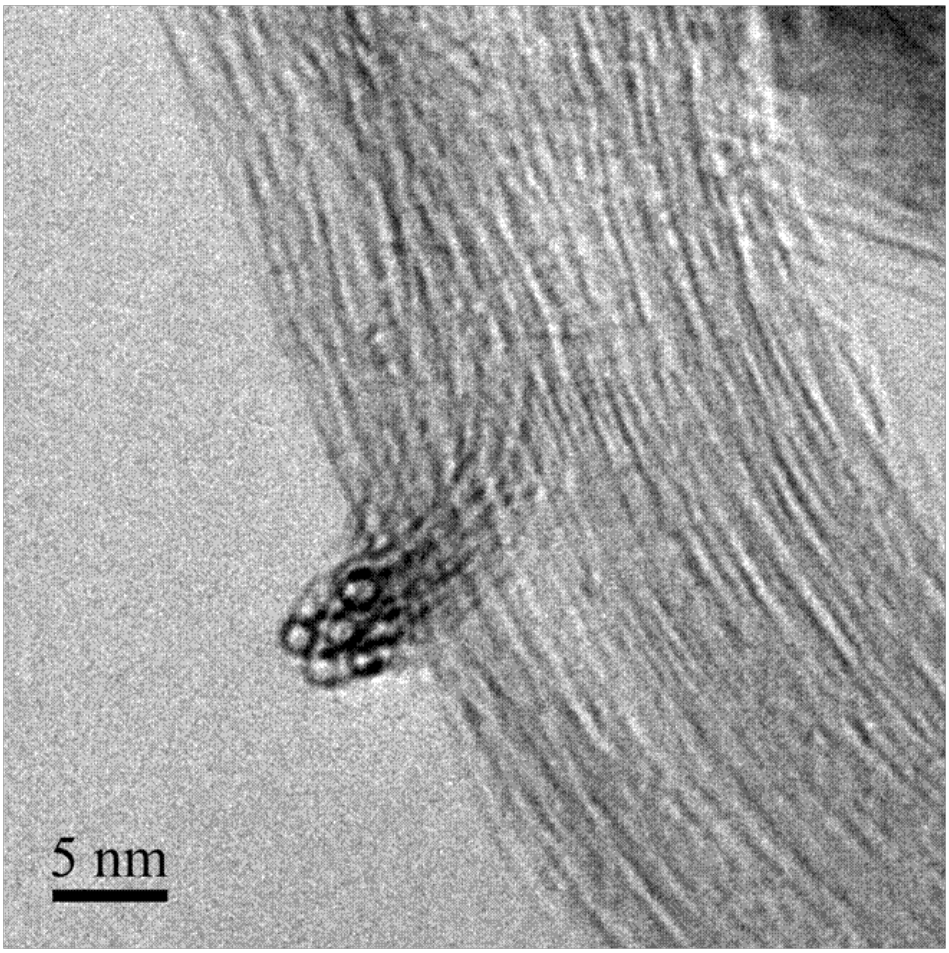

Figure 2: TEM image showing cross-sectional image of "rope"/"bundle" of SWNTs synthesized via the MGPx process

Along with the standard "R" grade material, another grade of HiPCO material referred to as "P" grade was also provided to BSI. "P" grade HiPCO is a purified form of the HiPCO "R" grade material that Unidym can provide. Although this material is not at the level of purification that BSI can produce, it was believed that it would make the BSI process more efficient since less rigorous acid treatment would be necessary. In addition, the special "P" grade HiPCO material contained tubes shorter than the norm, which would improve dispersibility and thereby facilitate type separation.

Synthesis experiments using the MGPx process was conducted in which one-wall nanotube synthesis was attempted using three different types of catalyst. The diameter distributions of these nanotube samples were measured using cross-sectional TEM (transmission electron microscope) images (figure 3). The median diameter of the one-wall nanotubes synthesized using the MGPx process is approximately 1 nm, which is comparable to that of HiPCO SWNTs. Figure 4 shows cumulative distribution functions comparing the diameters of HiPCO and three different batches of MGPx one-wall

nanotubes, CH3A-0234, CH3A-0235 and CH3A-0236, synthesized using different catalyst formulations. CH3A-0234 and CH3A-0235 were approximately 75% one-wall nanotubes and 25% two-wall nanotubes while CH3A-0236 was more than 95% one-wall nanotubes with the remainder being two-wall nanotubes. Therefore, by changing the catalyst formulation, the proportion of one-wall nanotubes to two-wall nanotubes can be controlled.

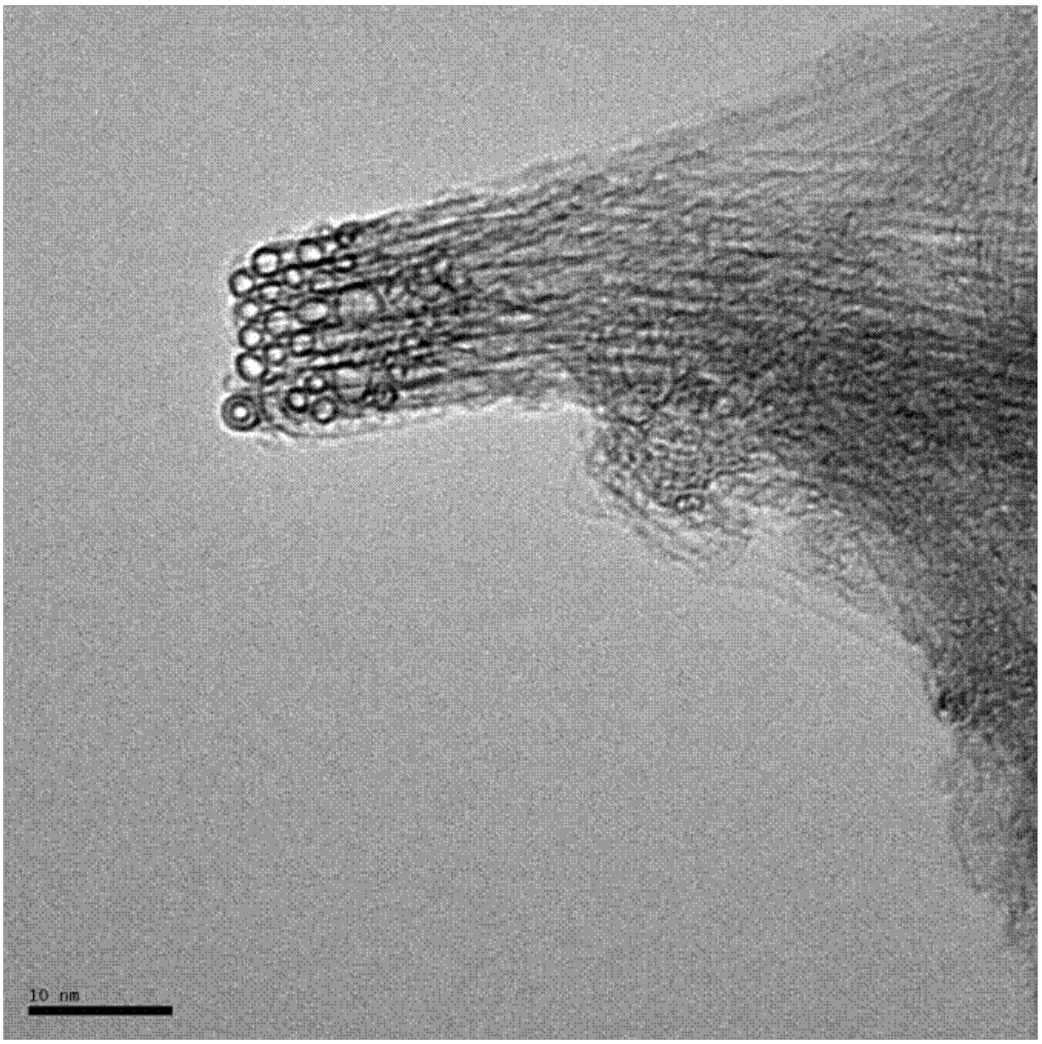

Figure 3: TEM image showing cross-sectional image of "rope"/"bundle" Buckytubes synthesized via MGPx process; the majority of which are one-wall nanotubes. Median diameter of MGPx tubes in this particular sample was approximately 1 nm.

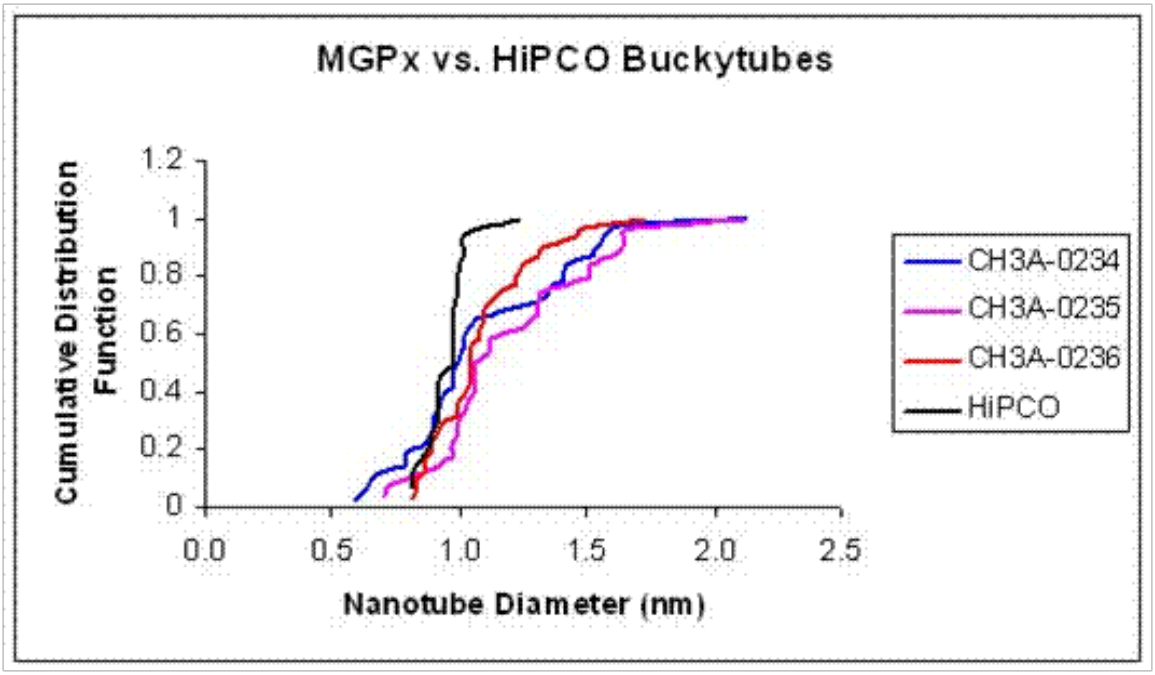

Figure 4: Cumulative distribution functions comparing diameters of MGPx and HiPCO one-wall nanotubes. Median diameters of MGPx and HiPCO tubes were 1.1 and 1 nm, respectively.

A number of different growth parameters for "R" grade HiPCO material was also produced. Three different materials, HPR180.1, HPR183.2 and HPR183.3 were produced and provided to BSI. For ease of handling, the tubes were delivered in four (4) 0.5 g aliquots for each material. These tubes were synthesized at temperatures that deviated from that used to synthesize standard HiPCO tubes; their synthesis temperatures are summarized in Table 1.

	Synthesis Temperature	**Catalyst**
HPR180.1	770 C	Fe + Co*
HPR183.2	1029 C	Fe + Co*
HPR183.3	944 C	Fe + Co*

Table 1: HiPco material synthesis at different temperature
*Amount of Co detected in final product was negligible (less than 0.05 at. % by EDS)

It was hypothesized that tube synthesis at temperatures lower than standard would result in a higher proportion of defects on the buckytube walls, thus facilitating functionalization and, therefore, dispersibility and stability in water. The high temperature synthesis material was provided for contrast. Comparison of TEM micrographs of HPR180.1 and HPR183.2 (figure 5) showed no significant differences in the materials were evident at medium magnifications (100K). However, TEM micrographs of HPR180.1 and HPR183.2 (figure 6) at high magnification (250K) appeared to indicate that the high temperature material was slightly "cleaner", i.e. contained less non-tubular carbon, particularly on the tube walls, than the low temperature material.

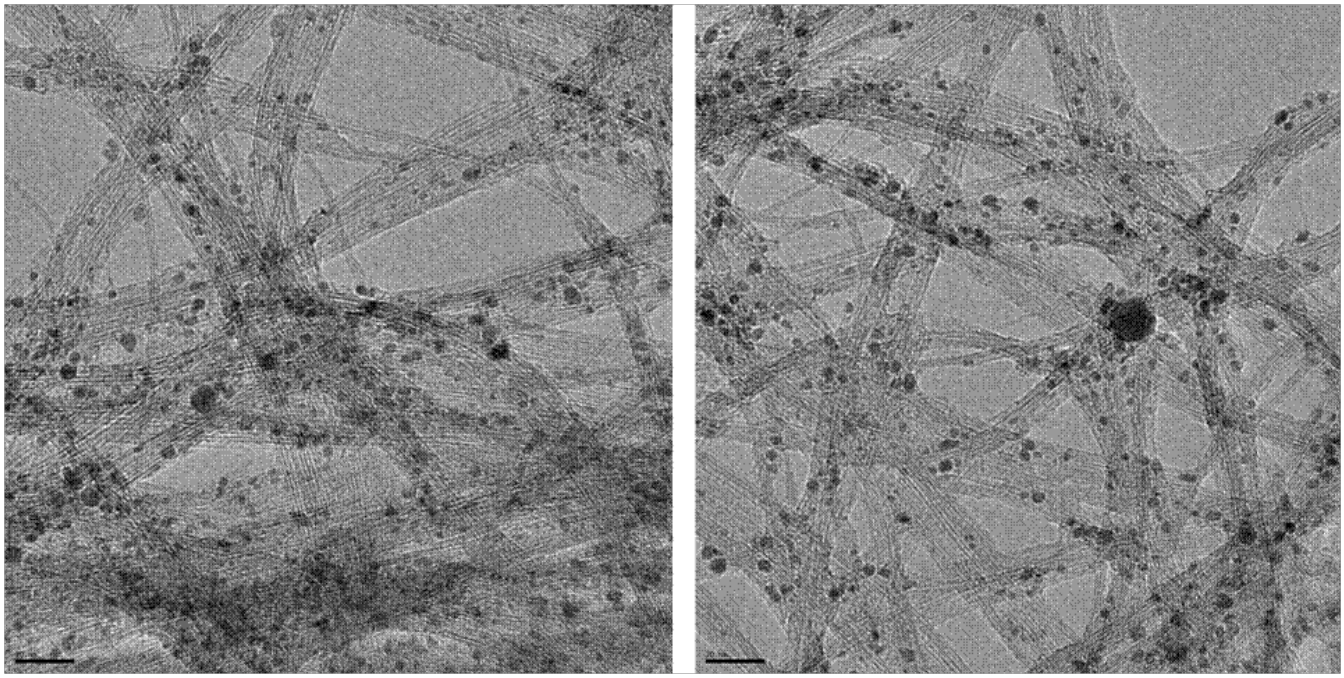

Figure 5: TEM micrographs of HPR180.1 (left) and HPR183.2 (right). Scale bar = 20 nm. At 100K magnification, differences, if any, between the two materials are not evident. In both materials, fringe lines in the nanotube ropes are clear enough to be visible at medium magnifications. The dark particles are metal catalyst particles.

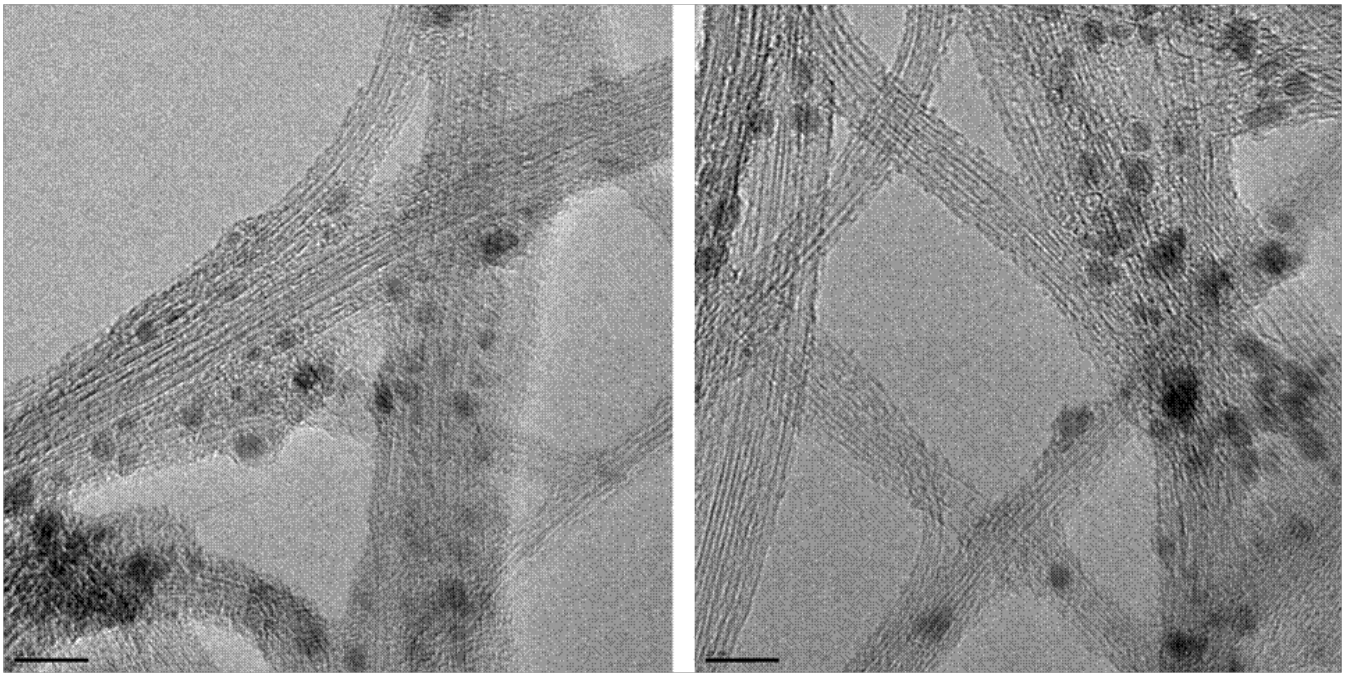

Figure 6: TEM micrographs of HPR180.1 (left) and HPR183.2 (right). Scale bar = 10 nm. At magnifications higher than 100K, fringe lines in TEM micrographs of HPR183.2 appear to be marginally cleaner than those in HPR180.1, possibly indicative of less non-tubular carbon coating tubes and ropes.

1.3.2.2 Alternative Diazonium Salt Type-Separation Method

In addition to providing HiPCO SWNTs to BSI, Unidym had been active in carrying out its own semiconductor enrichment work. Standard HiPCO tubes were reacted with a diazonium salt solution in an attempt to synthesize semiconductor SWNTs (s-SWNTs). Upon reaction with the diazonium salt solution, dramatic changes occur in the Raman profiles of the SWNT solutions. Figure 7 shows the Raman profile for a SWNT solution after it has been reacted with a 1000 microliter aliquot of diazonium salt solution.

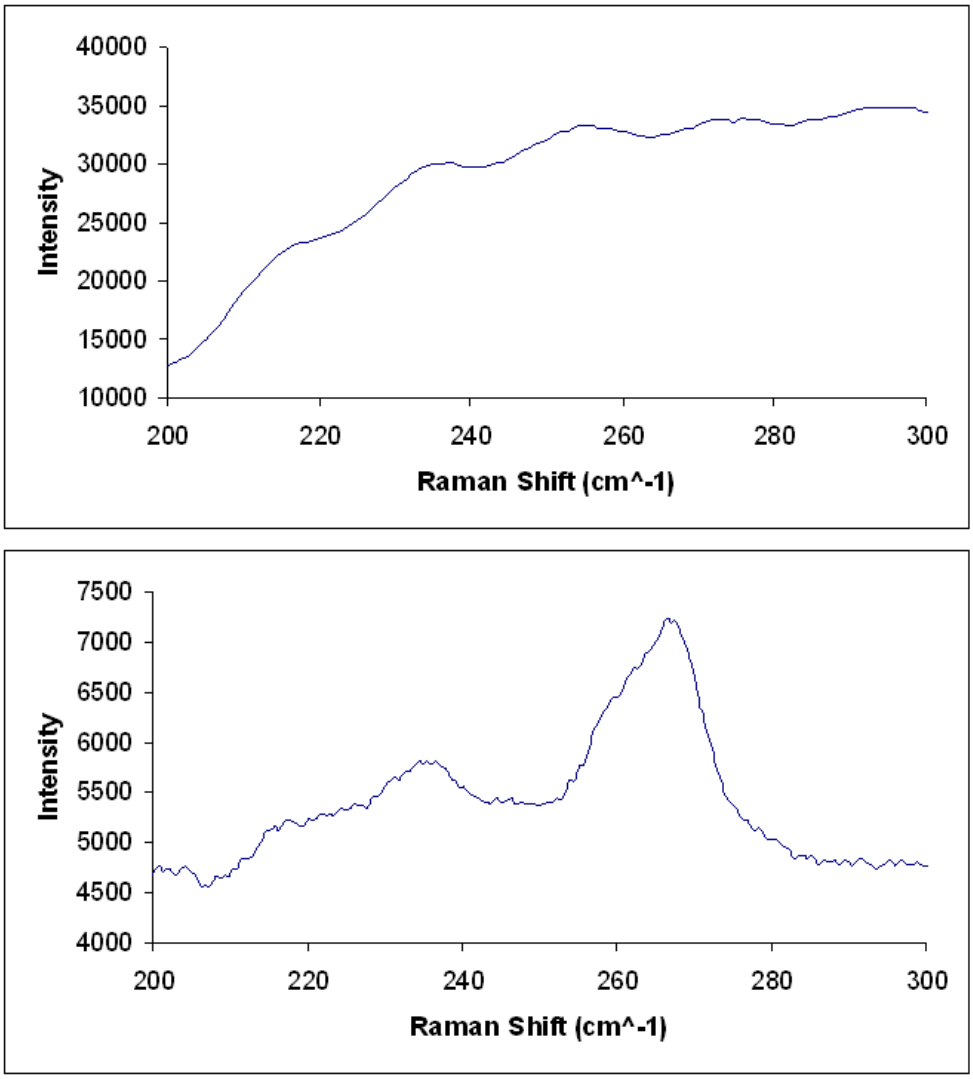

Figure 7: Raman profiles for SWNT solution reacted with 1000 microliters of diazonium salt solution, centered around the RBMs. The top profile was measured using a 633 nm laser. The bottom profile was measured using a 785 nm laser.

Under a 633 nm laser, the observable RBM's can originate from either semiconducting or metallic SWNTs assuming a diameter range typical of HiPCO tubes. Under a 785 nm laser, the observable SWNTs with diameters typical of HiPCO tubes are semiconductors. Thus, the elimination of the RBMs observable under a 633 nm laser and the persistence of the RMB's observable under the 785

nm laser appear to give some evidence of semiconductor enrichment after the reaction of HiPCO SWNTs with a diazonium salt solution.

Further evidence of semiconductor enrichment is provided by measuring the change in the electronic transport properties of the HiPCO nanotubes upon doping. Assuming a statistical average of the distribution of the possible chiralities given a nanotube diameter, one would expect 33% of the tubes to be metallic and the remaining 67% to be semiconducting. The addition of charge carriers to the metallic tubes would have an egligible effect on their resistance while the effect on semiconducting tubes would be dramatic.

Films were made of different "inks", each reacted with different levels of diazonium salts. The solutions were filtered through anodisc 20 nm pore size filters and washed with 200 mL of DI water. Once the films were dry, leads were painted onto them using silver paint/epoxy. The resistance of the films was measured with a Keithley 2400 and measured in-situ while they were p-doped with NO_2 gas. Figure 8 shows the ratio of the initial film resistance to film resistance after NO_2 doping versus the concentration of the diazonium salt solution added to the SWNTs.

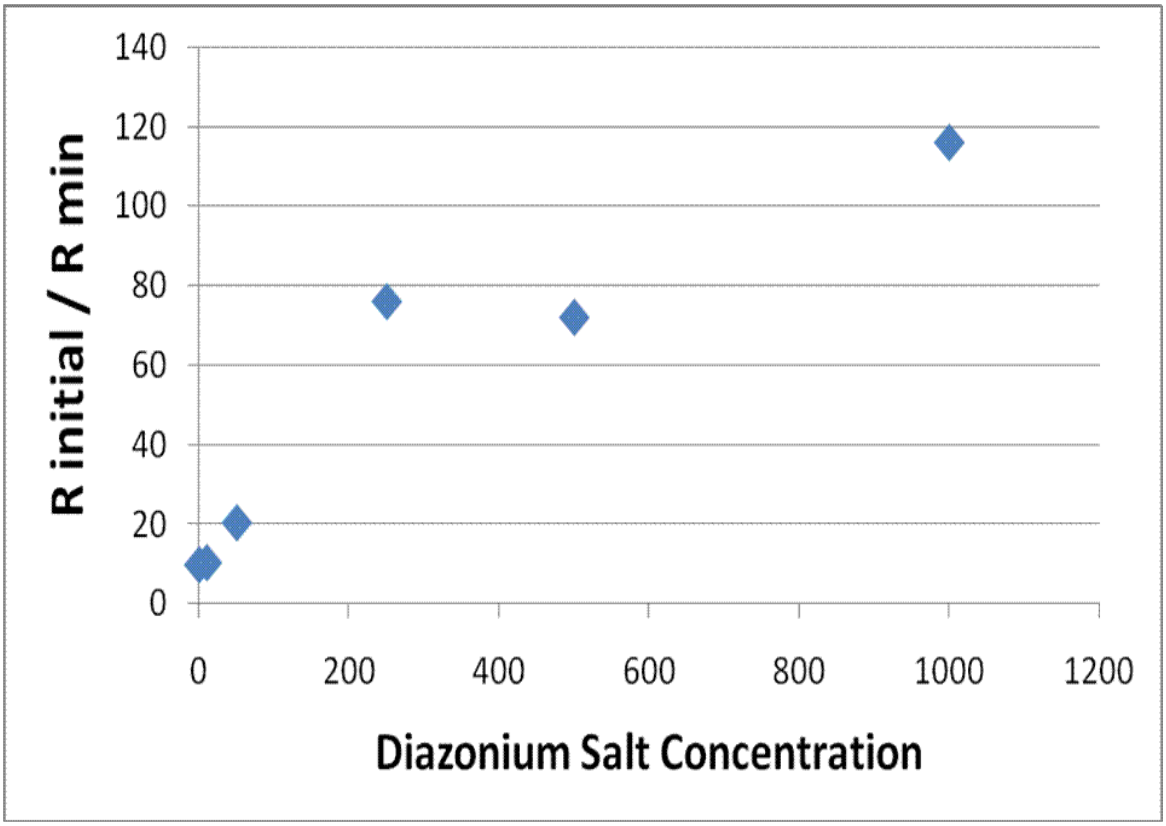

Figure 8: The ratio of initial resistance to resistance after NO_2 doping versus the diazonium salt concentration of the initial "inks". The rise in the resistances ratio upon addition of diazonium salts to the HiPco tubes in solution supports the conclusion that the reaction of diazonium salts and SWNTs results in semiconductor enrichment.

A correlation is seen as the effect of NO_2 doping increases with an increase in the amount of diazonium salts added to the SWNTs increases. For characterization of the diazonium salt treated material, a SWNT based transistor was fabricated and then characterized. Figure 9 shows the on/off ratio

vs. the density of the carbon nanotubes. The typical on/off ratio for a nanotube network transistor is around 1000, which is much too small. One obvious route to improve the on/off ratio is to "kill" the metallic nanotubes chemically or electronically; typical avenues of achieving this goal are via diazonium functionalization or electrical breakdown.

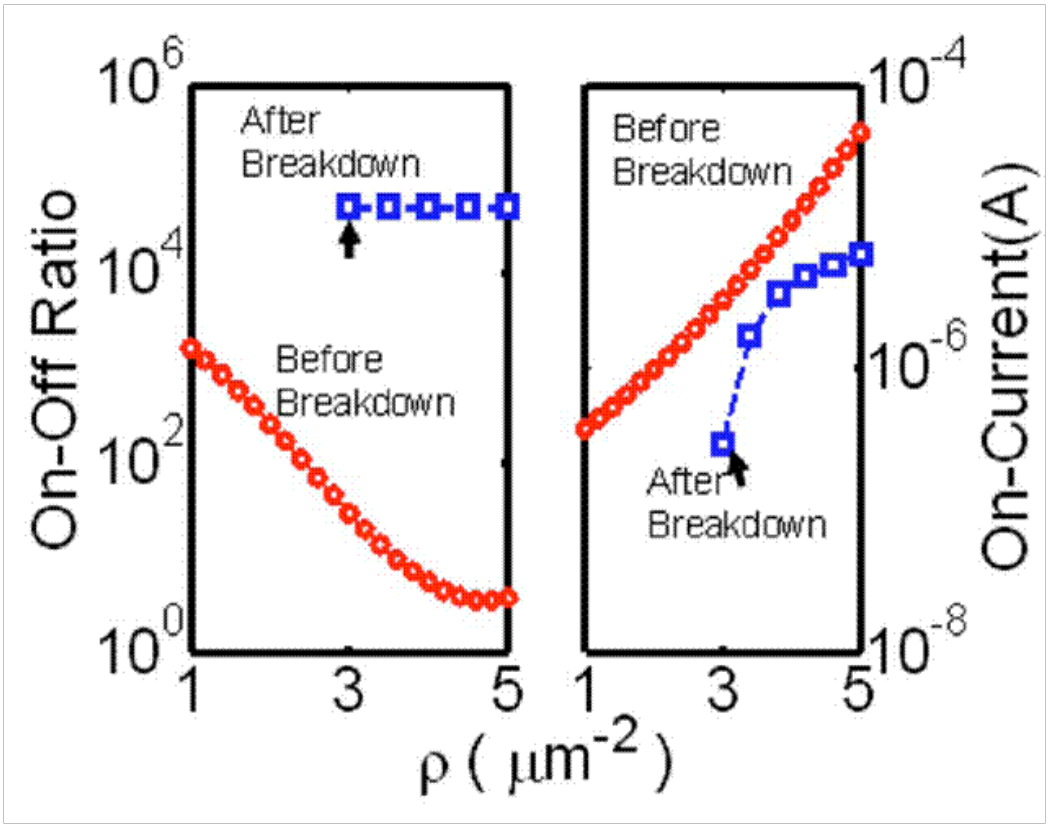

Figure 9: Dependence of on/off and on-current on the nanotube density before and after electrical breakdown.

The transistor device that was made is depicted in the schematic shown in figure 10. The channel width is 1000 μm and the channel length varies from 5 μm to 500 μm. The transistors' transfer characteristics are measured with one Keithley 2400 for applying V_{sd} and measuring I_{sd} and another voltage source to apply the gate voltage. The applied V_{sd} = 100 mV and the gate voltages sweeps with a step of 0.5 V.

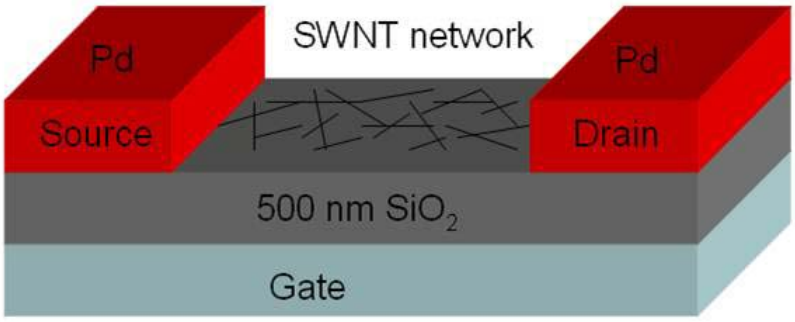

Figure 10: Transistor structure with CVD-grown SWNT network on a SiO_2 as channel and Pd as source/drain contacts.

Figure 11 shows a typical transfer curve of a nanotube network transistor with a 500 µm channel length. The mobility is calculated with equation 1 and is found to be 5 cm/V s. Note that the device shows a large hysteresis, which may be due to trapped water molecules or charge build-up at the SiO_2/nanotube interface

$$\mu = \frac{l}{w}\frac{\mathrm{d}I_{\mathrm{sd}}}{\mathrm{d}V_g}\frac{d}{k\epsilon_0}\frac{1}{V_{\mathrm{sd}}} \qquad (1)$$

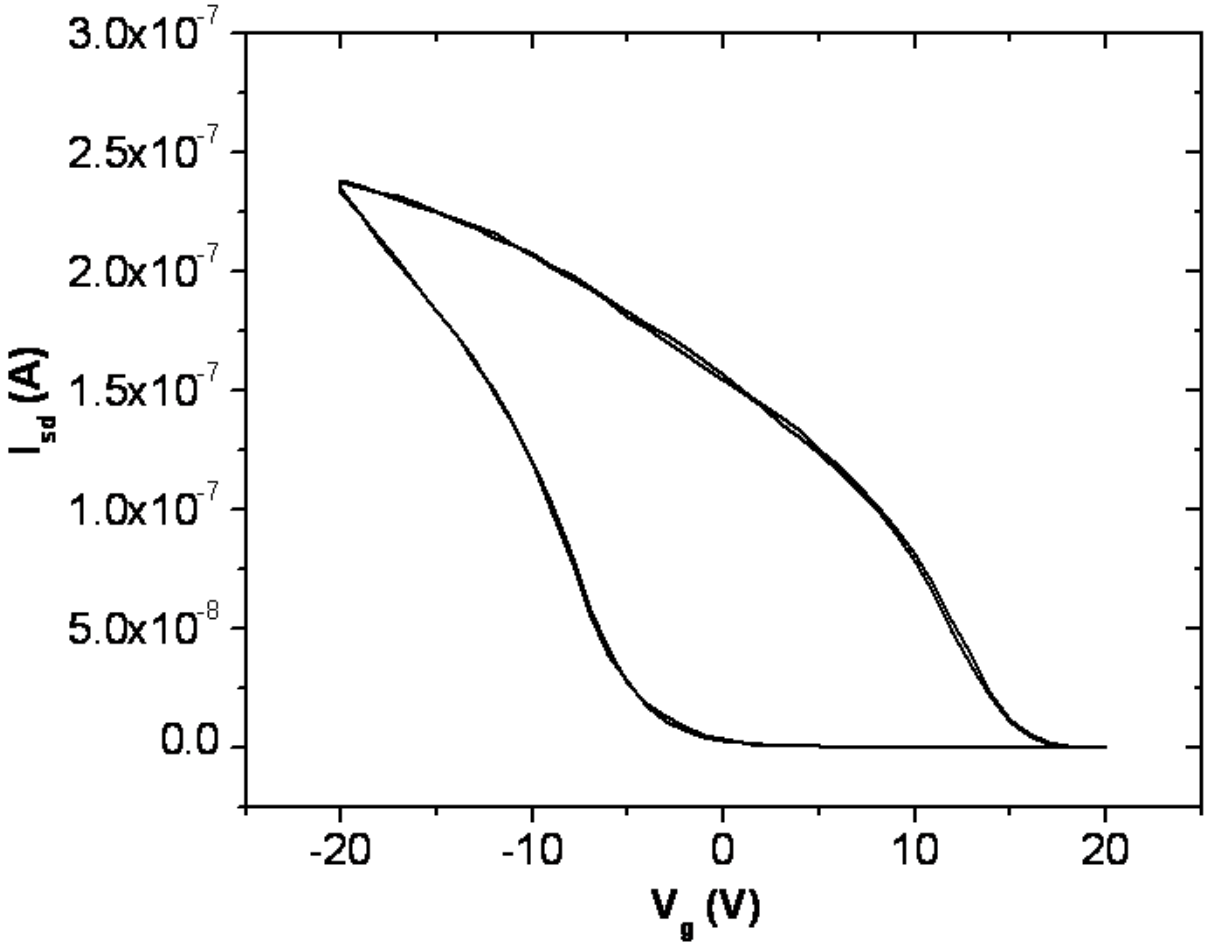

Figure 11: A typical transfer curve of CVD-nanotube network transistors on silicon substrates.

1.3.3 Subcontractor: Brewer Science, Inc. Task Summary

1.3.3.1 Buckytube Refinement and Purification

For BSI's portion of the project, the work involved further processing of the as-produced HiPCO "R" grade SWNTs provided by Unidym to remove metallic catalysts and carbonaceous contaminants. The second task was to take the as-produced SWNTs and disperse them in either a surfactant based aqueous solution or functionalizing (purifying) via acid-treatment to produce a surfactant-free aqueous solution for the purpose of metallic and semiconducting nanotube separation using dielectrophoresis. Initial studies into type-separation included development of a simple inter-digit micro-array electrode system, which was connected to an AC signal generator. By providing an AC signal between conducting electrodes it was demonstrated as shown in the scanning electron microscopy (SEM) image in figure 12, that the metallic SWNTs (m-SWNTs) align themselves perpendicular to the length of the parallel electrodes. These initial studies were conducted on electrodes that were 150µm apart and therefore alignment of the tubes was not significant, therefore electrode geometry optimization was necessary, which will be discussed in more detail in the next section.

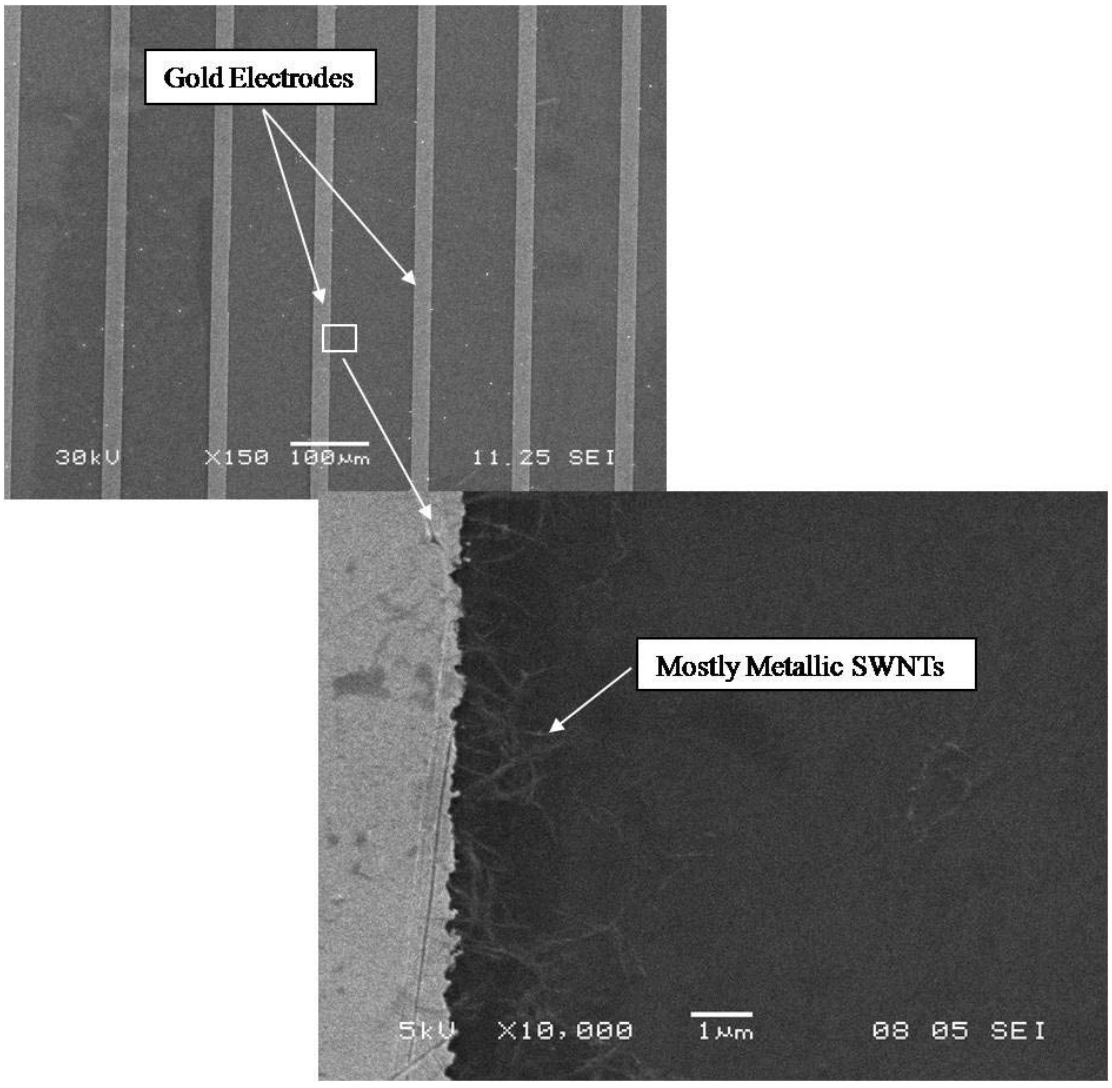

Figure 12: SEM image of Au electrodes with m-SWNTs aligned along the electrode.

Raman photospectroscopy was used to characterize/compare the SWNT solution pre-dielectrophoresis (Pre-DEP), post-dielectrophoresis (Post-DEP), as well as the SWNTs extracted by the electrode. It was found that relatively higher m-SWNT content was deposited between the electrodes as opposed to that of the pre-separated solution. Relatively higher s-SWNT content was found in the Post-DEP solution as compared to that of the Pre-DEP solution. Although these preliminary results were positive and encouraging, further refinement was required to optimize the entire process.

1.3.3.1.1 SWNT raw materials processing

The materials received from Unidym of different grades and batches were processed using different chemical treatments. Raman analyses were conducted on these materials and compared to those obtained from the SWNTs solutions derived from these raw materials. It was found that the dispersion characteristics of each material were different and consequently, the purification process needed to be tailored accordingly. It was concluded that the inconsistency of the raw material had a detrimental impact on the effectiveness of a set purification process to produce consistently performing SWNT solution products.

Various SWNT materials were provided by Unidym, which were produced under different conditions, specifically using different growing temperatures and reactor set-ups. In addition, the HiPCO materials came in three different forms: as-produced fluffy, mud (wet cake), and granular (sand). The wet cake contained more than 98% water, and the granular SWNT materials were freeze-dried after the as-produced SWNT material had gone through certain treatment steps. The as-received HiPCO materials were dispersed into liquid form with appropriate media, such as water or organic solvents. For purifying the as-received materials, an aqueous media is required.

A total of 12 batches of HiPCO materials, with different growing parameters, was obtained and processed. The three forms of as-received HiPCO raw materials possessed different handling characteristics. The granular (sand) and mud (wet cake) were easier to handle than the fluffy powder materials. The fluffy material was very difficult to handle due to its feather-light characteristics. The as-received HiPCO materials were handled inside a glove box for weighing and converting into liquid form with appropriate media, such as water or organic solvents, to prevent personnel from being exposed to SWNTs. The liquid form solutions were then processed accordingly. For purifying the as-received materials, aqueous media was used. The as-received HiPCO materials were characterized using atomic force microscopy (AFM) to determine nanotube length and thermogravimetric analysis (TGA) to detect residual substances (mostly metal impurities) in the materials and to determine the decomposition onset temperature. Some were characterized using UV-VIS photospectrometer. The SWNT mean length ranged from 469 to 1420 nm and median length ranged from 352 to 1315 nm. The HiPCO materials, due to different growing parameters, had a very wide range, specifically, 8% to 48%, of residual (metal) content. It was observed that the highest residual content material aggregated around the magnetic stirring bar at the very beginning of the purification process. These analytical results are summarized in Table 2.

SWNT Batch	**Received Amount**	**Information**	**Form**	**Length (AFM) (nm)**	**TGA**	**UV-Vis**	**Dispersion characteristics (with BSI process)**	**Approximate Stability of purified/ dispersed product**
R0558	Purchased 8/3/07	HiPCO tubes, standard process	Fluffy powder	Median: 495 Mean: 742	Residual: 29% T_{onset} ~340 ˚C		Easily dispersed. Final product: OD>3 possible	Stable for >6 months
R0559	Purchased 8/3/07	HiPCO tubes, standard process	Fluffy powder	Median: 1164 Mean: 831	Residual: 22% T_{onset} unknown		Moderate dispersibility. Final product: OD>3 possible	Stable for several months
R0546	Purchased 1/4/08	HiPCO tubes, standard process	Fluffy powder	Median: 352 Mean: 597	Residual: 25% T_{onset} unknown		Moderate dispersibility. Final product: OD~3 possible	Stable for several months
RR183.5	Received 8/8/08	HiPCO tubes, standard process	Fluffy powder	Median: 579 Mean: 1003	Residual: 26.5% T_{onset} ~400 ˚C	√	Difficult to disperse. Final product: OD~1.9 possible	Stable for several days
ATP035	Received 9/9/08	*Purified (post processed)* HiPCO tubes	Fine sand free-flowing powder	Median: 1315 Mean: 1416	Residual: 11.3 % T_{onset} ~400 ˚C	√	Difficult to disperse. OD 2.7 obtained.	OD=2.7 Stable for 1 day. OD= 1.89 stable for ~ 1 week
R0238	10/08/08	HiPCO tubes, treatment with EtOH post synthesis	Sand	Median: 379 Mean: 469	Residual: 48% T_{onset} ~350 ˚C	√	Extremely difficult to disperse. OD~2.2 obtained	Uncentrifuged sample stable for 2 days (OD=2.2). Centrifuged sample stable for > 2 weeks (OD=1.49)
P0356	11/13/08	*Purified* HiPCO tubes	Fine sand free-flowing powder	Median: 531 Mean: 677	Residual: 8% T_{onset} ~340 ˚C	√	Not possible to disperse under standard conditions	NA
TST178-1	12/26/08	MGPx process (rich in SWCNT's, made with low cost metal cat.)	Mud		Residual: 21.7% T_{onset} ~420 ˚C		*Abandoned* - process may not be reproducible at this time	NA
HPR179.2	12/26/08	"In kind" tubes made with new HiPCO reactor	Fluff		Residual: 21.7% T_{onset} ~300 ˚C		Not possible to disperse effectively under standard conditions	NA
SWCNT Batch	**Received Amount**	**Information**	**Form**	**Length (AFM) (nm)**	**TGA**	**UV-Vis**	**Dispersion characteristics (with BSI process)**	**Approximate Stability of purified/ dispersed product**

HPR180.1	1/4/09	Synthesized at 770 ˚C	Fluff		Residual: 19% T_{onset} ~400 ˚C		Difficult to disperse	Difficult to disperse, unstable
HPR183.2	1/4/09	Synthesized at 1029 ˚C	Fluff		Residual: 33% T_{onset} ~380 ˚C		Extremely difficult to disperse. OD~0.4 obtained	Stable for 1 day
HPR183.3	1/4/09	Synthesized at 944 ˚C	Fluff		Residual: 21% T_{onset} ~380 ˚C		In progress	

Table 2: Basic information and characterizations of all batches of HiPCO raw materials and purified SWCNT solutions characteristics.

1.3.3.1.2 Purification of HiPCO raw materials

The purification process for SWNTs mainly involved a series of chemical treatments (typically an acid reflux process and BSI's proprietary chemical treatment processes), pH adjustment, sonication, filtration, and centrifugation steps. Each step involved extensive and precise processing control. The steps were also inter-related and required close attention to improve processing of the materials. A representative purification process flow is shown in Figure 13.

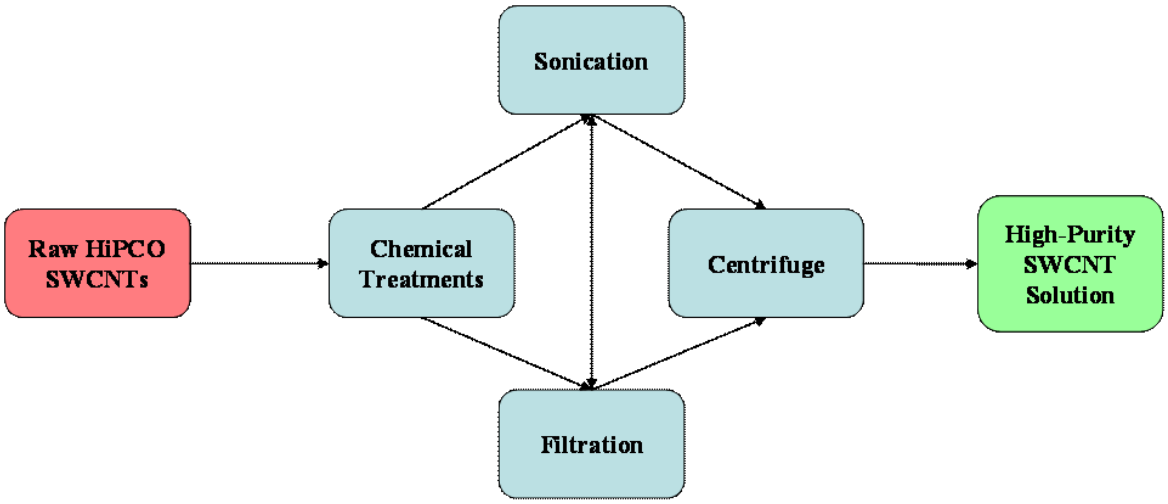

Figure 13: A representative schematic SWNT purification process.

The HiPCO SWNT is first weighed and dispersed into deionized water, and then sonicated to exfoliate the bundled SWNTs prior to any further processing. The solution is acidified to a certain pH or concentration using various acids such as nitric acid, sulfuric acid, and hydrochloric acid. The main purpose of this acid reflux step is to digest the metallic nanoparticulates and carbonaceous impurities as well as break down the SWNT tips to digest the metal nanoparticulates encapsulated inside them.

The refluxed solution was then subjected to proprietary chemical treatments and then subjected to filtration to remove digested metal (from metal nanoparticulates) and oxidized carbonaceous impurities. Subsequently, a specially designed filtration system is deployed for removing the digested metal and carbonaceous impurities from the SWNT solution. This system also provided a means to concentrate the nanotube solution, if necessary. The permeate and retentate are characterized for their optical densities (ODs) using a UV-VIS spectrometer. This technique is used to determine if the carbonaceous impurities have been removed from the solution, as well to determine the relative CNT concentration. Overall, it was found that the as-produced fluffy HiPCO material was easier to disperse and purify.

1.3.3.1.3 Characterization of purified SWNT solutions

The purified SWNT solutions were characterized using Raman spectroscopy for the appearance of SWNTs with different diameters and electronic characteristics (metallic or semiconducting), as well as to detect the presence of carbonaceous impurities and/or defect levels. Scanning electron microscopy (SEM) and Atomic Force Microscopy (AFM) were used to characterize the deposited SWNTs for coating quality, carbonaceous impurity, and SWNT length.

Raman spectroscopy equipped with a 632.8-nm wavelength laser was used to characterize the purified SWNT materials for the appearance of G (1540 cm^{-1} to 1600 cm^{-1}), D (about 1330 cm^{-1}), and RBM (radial breathing mode, about 100 cm^{-1} to 400 cm^{-1}) bands, as shown in figure 14. A small volume of SWNT solution is filtered on a ~ 2-inch-diameter filter disk and dried. This filter disk was then characterized using the Raman spectroscopy. A typical doublet tangential mode (G^+ and G^- bands), which indicates the existence of SWNTs, is clearly observed. The observation of the disorder-induced mode (D band) indicates either the presence of defects on nanotube surfaces and tube ends or the presence of carbonaceous impurities. It also can be caused by the carboxylic functional groups on the nanotubes after the acid-reflux purification process. The presence of the RBM bands is a characteristic unique to CNTs which is not observed in other carbonaceous materials.

The electrical characteristics of the SWNTs, that is, metallic and semiconducting, can be identified according to the Kataura plot in figure 15. Also, as shown in figure 15, the Raman shift at about 194 cm^{-1} is identified as m-SWNTs, while the s-SWNTs contributed to the Raman shift at about 258 cm^{-1}. The peak at about 218 cm^{-1} is also identified as m-SWNTs however; it is debatable as to whether or not the peak is caused by bundled SWNTs of m- & s-SWNTs. When different wavelengths of laser light are used in the Raman spectrometer, they will resonate with different diameters, therefore, different chiralities of SWNTs.

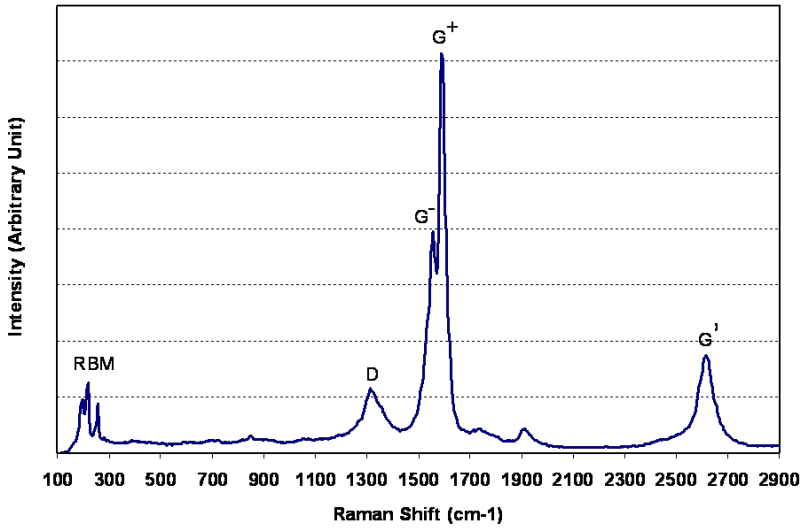

Figure 14: A representative Raman spectrum obtained from the purified SWNTs on a filter disk. The radial breathing mode (RBM; 100 cm^{-1} to 400 cm-1), disorder-carbon (D; about 1330 cm^{-1}), and tangential (G; about 1540 cm^{-1} to 1600cm^{-1}) modes are labeled.

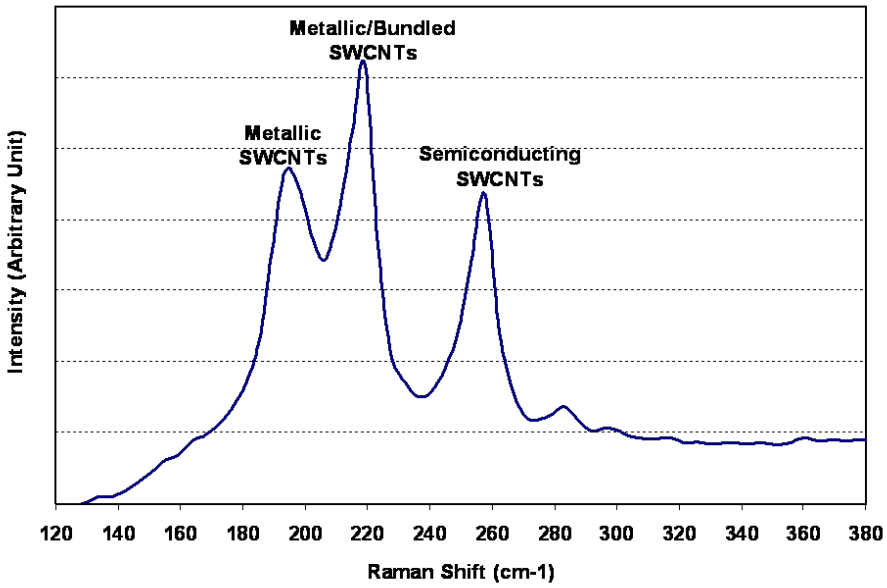

Figure 15: SWNT radial breathing mode (RBM) Raman shifts within the range of 120 cm^{-1} to 380 cm^{-1} in Figure 2.

SEM and AFM were used to complement Raman spectroscopy for characterizing the purified SWNT material. In figure 16(A), SEM characterization indicates a very dense SWNT fabric coated onto a silicon wafer surface with little or no carbonaceous impurities (mostly amorphous carbon). Amorphous carbon blurs the nanotube images seen in the SEM micrographs. In addition, no noticeable particulate, which could also result from the spin-coating process, was observed across the SWNT fabric. AFM data shows the SWNT lengths ranging from a few tenths of a micron to greater than 2.5 μm; see figure 16(B). It was evident that the majority, if not all, of the carbonaceous impurities (mostly

amorphous carbon) were removed, as indicated by SEM and AFM characterization, after the purification process.

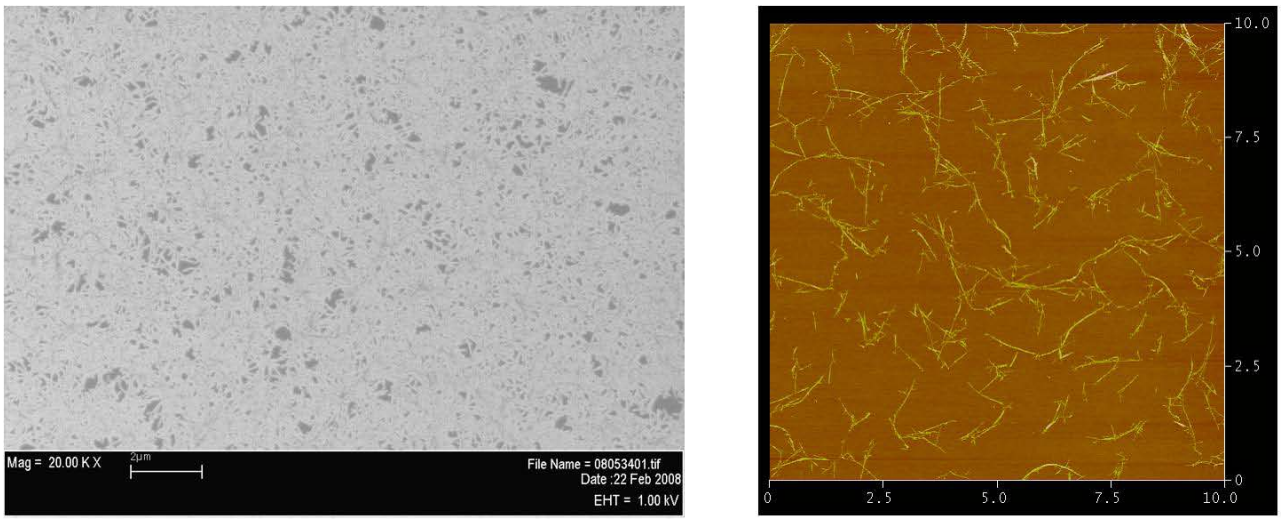

Figure 16: (A) SEM and (B) AFM micrographs of spin-coated SWNTs on silicon wafer substrates.

1.3.3.2 Buckytube Type-Separation via Dielectrophoresis

Dielectrophoresis was used to separate metallic and semiconducting SWNTs in aqueous media. Both as-produced and purified SWNT solutions were used to demonstrate the feasibility of using this separation technique. This work was carried out using a small cell (steady solution) dielectrophoresis setup for the initial proof-of-concept. As-produced SWNT material was dispersed into aqueous media and another SWNT solution was prepared through the purification process. Both solutions were used for metallic and semiconducting nanotube separation using dielectrophoresis. Simple small inter-digit array electrodes, about 1 cm x 1 cm, were fabricated on a silicon oxide wafer for initial proof-of-concept purposes. The electrodes were fabricated with Cr/Au coating on the silicon oxide wafer with photolithography, wet chemical etching, and resist stripping processes. The wafer was diced to produce an individual electrode. The individual electrode was connected with an AC signal generator and approximately 400µL of SWNT aqueous was placed on the electrode, and an AC signal was applied. SWNTs were found on the electrode after the dielectrophoresis process as was shown in the initial results in figure 17.

Raman photospectroscopy was used to characterize the SWNT solution Pre-DEP and Post-DEP, as well as the SWNTs extracted by and adhered between the electrodes. The HiPCO SWNTs were dispersed into deionized water using one of two methods; surfactant or purification to study both pre and post purification solutions after the dielectrophoresis process was carried out. The SWNT solution that was extracted and SWNT material that adhered to the electrodes was also characterized using a Raman spectroscopy, as shown in figure 17. It also shows the Raman spectra for the pre-purified SWNT solution, which clearly reveals that the relative peak intensity and area ratios for m-SWNTs and s-SWNTs have changed drastically for those SWNTs extracted from the electrode as opposed to those from the as-produced SWNT solution. The decrease in s-SWNTs on the electrode is evident, as indicated by the decrease in the relative intensity of the s-SWNT peaks (256, 258, and 284 cm^{-1}) compared to those obtained from the as-produced SWNT solution, while the m-SWNT peak (197 cm^{-1}) remains constant.

The same study was done on the acid-treated (purified) SWNT aqueous solution and a subsequent Raman study was carried out as shown in figure 18. The Pre-DEP and Post-DEP SWNT solutions have very similar Raman spectrum profiles. This is due to the relative larger amount of the solution used for dielectrophoresis. However, the SWNTs on the electrode possess a very different Raman spectrum profile, as clearly seen in Figure 18. The s-SWNT peak intensity at 257cm^{-1} and 284 cm^{-1} is reduced greatly while the m- SWNT peak intensity at ~196 cm^{-1} remains constant. This indicates that the SWNTs on the electrode are predominantly m-SWNTs after dielectrophoresis.

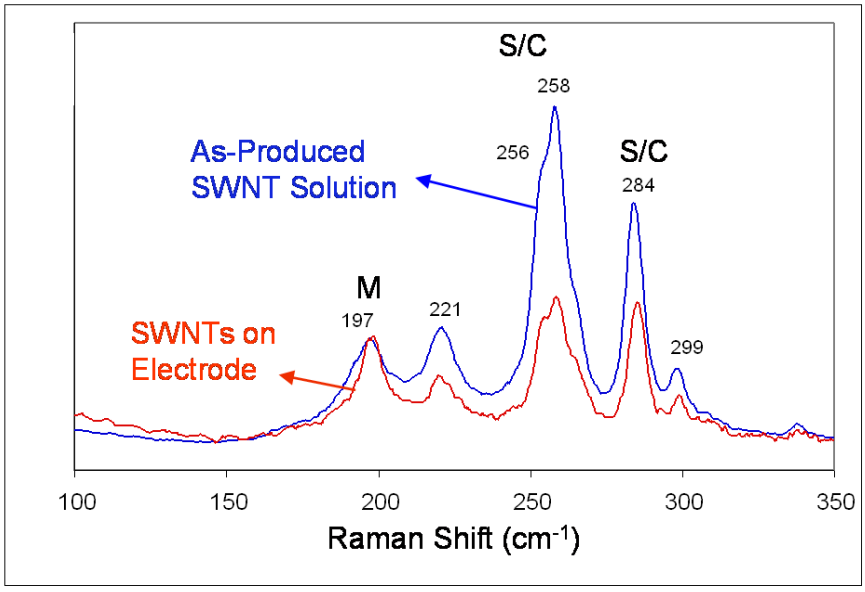

Figure 17: Raman spectra (633-nm laser) of the as-produced SWNT solution and the SWNTs adhered onto the electrode Post-DEP.

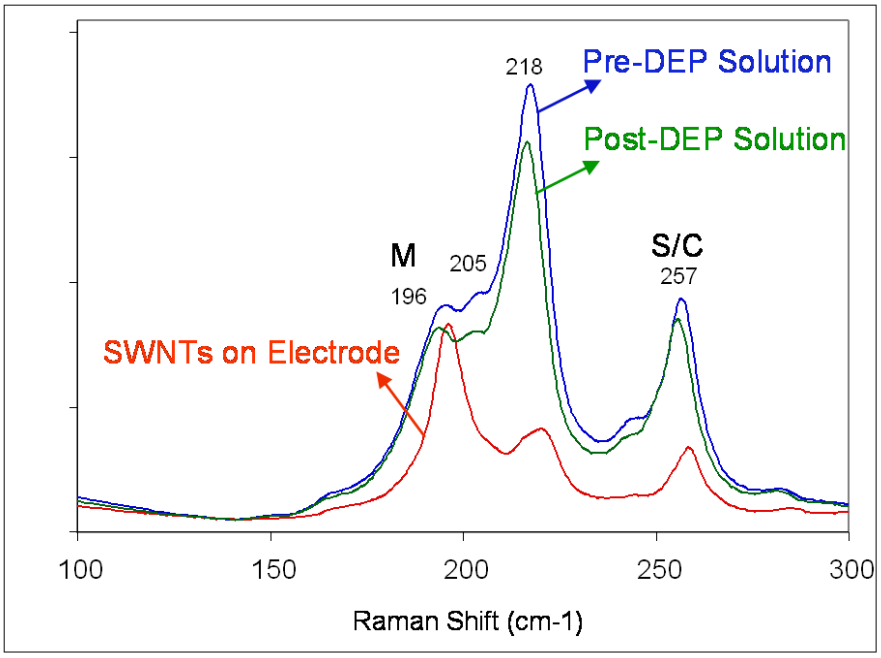

Figure 18: Raman spectra (633 nm laser) of the Pre-DEP and Post-DEP SWNTs and the SWNTs adhered to the electrode after dielectrophoresis.

A continuous flow dielectrophoresis cell and electrode as shown in figure 19 was designed and fabricated as part of the SWNT separation scale-up effort. The cell would be used to type-separate carbon SWNT solution in larger quantities. The m-SWNTs can be extracted from the electrode and re-dispersed into the appropriate solvent.

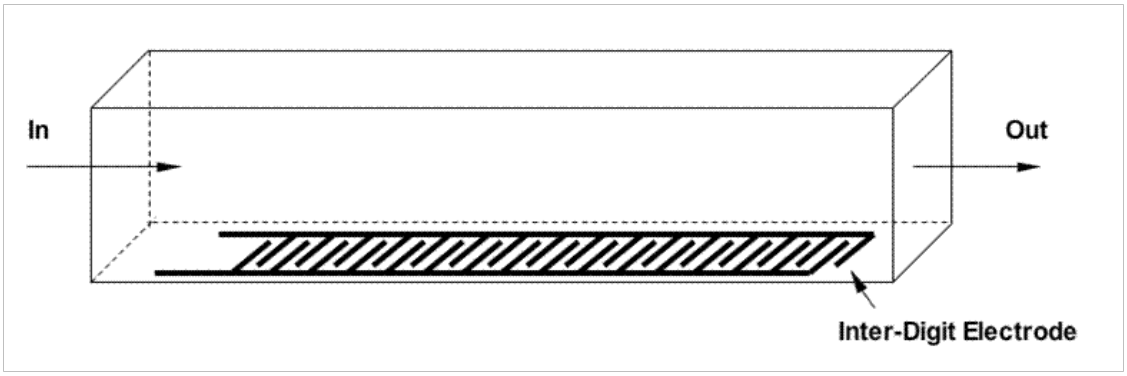

Figure 19: A continuous flow dielectrophoresis cell configuration with inter-digitated electrode array at bottom.

It was demonstrated that high-purity, surfactant-free SWNT aqueous solutions was developed using only 1 or 2 types of HiPCO SWNT material, and the process can be controlled and scaled up. From a mass production standpoint, both process controllability and raw materials consistency are required. A bench-scale dielectrophoresis process for separating m-SWNTs and s-SWNTs has been proven and developed, but still requires refinement.

1.3.4 Prime:JVIC-Missouri State University Task Summary

1.3.4.1 Identification of Electrical Properties of SWNTs

JVIC's task on this project was to provide overall management along with facilitation of materials electronic properties characterization as well as device application. JVIC also produced the electrode systems via photolithography that BSI required to perform the dielectrophoresis studies. It had been determined that apart from the basic room temperature 4-point IV and temperature dependent resistance measurements to electrically characterize the refined SWNT material, developing a number of device applications would allow for further electrical characterization.

In indentifying the electrical properties of the type-separated SWNT's, initial room temperature IV and temperature dependent resistance measurements were conducted on the Pre-DEP HiPCO SWNTs. This allowed for a baseline measurement to be conducted prior to type-separation which would establish a protocol for comparison with the Post-DEP SWNTs. HiPCO SWNT's were spin coated onto two oxide wafers; one was coated with 2 coats and the other was coated with 5 coats. The wafers were characterized for both room temperature IV as well as temperature dependant resistance measurements.

For test purposes 3 regions on the wafer (near edge 1, middle, & near edge 2) of a 100mm diameter wafer were cut out and measured for room temperature IV as well as temperature dependent resistance characterization. The dies where chosen along the diameter of the wafer as shown in figure 20. Since the SWNT solution was spin coated and the coating application is a radial effect, this would allow for a quick check to see the uniformity of the coat along the length (diameter) of the wafer. The IV plots for the 2 coat wafer for the three regions are shown in figure 21; the slope of the linear equation is the resistance of the SWNT material being measured. The same is shown for the 5 coat wafer in figure 22. It is evident that there is some slight non-uniformity along the diameter of the wafer but this method is sufficient as a quick check to determine the order of magnitude of the coated SWNT material when the electrical property comparisons of Pre-DEP and Post-DEP coated wafers are being made.

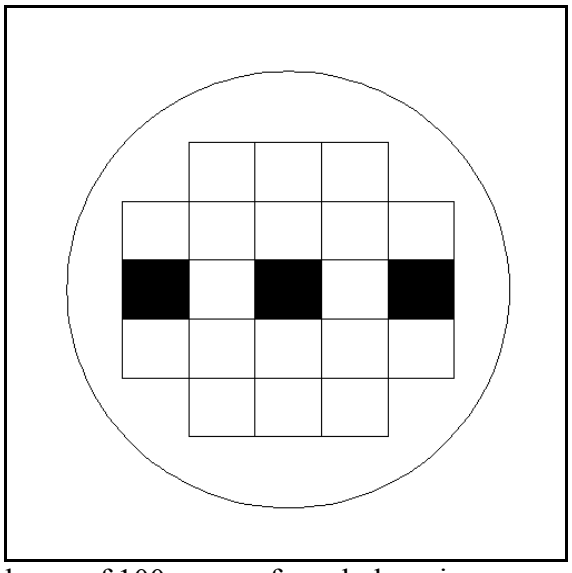

Figure 20: Die laser scoring scheme of 100 mm wafers; dark regions represent the 3 regions tested.

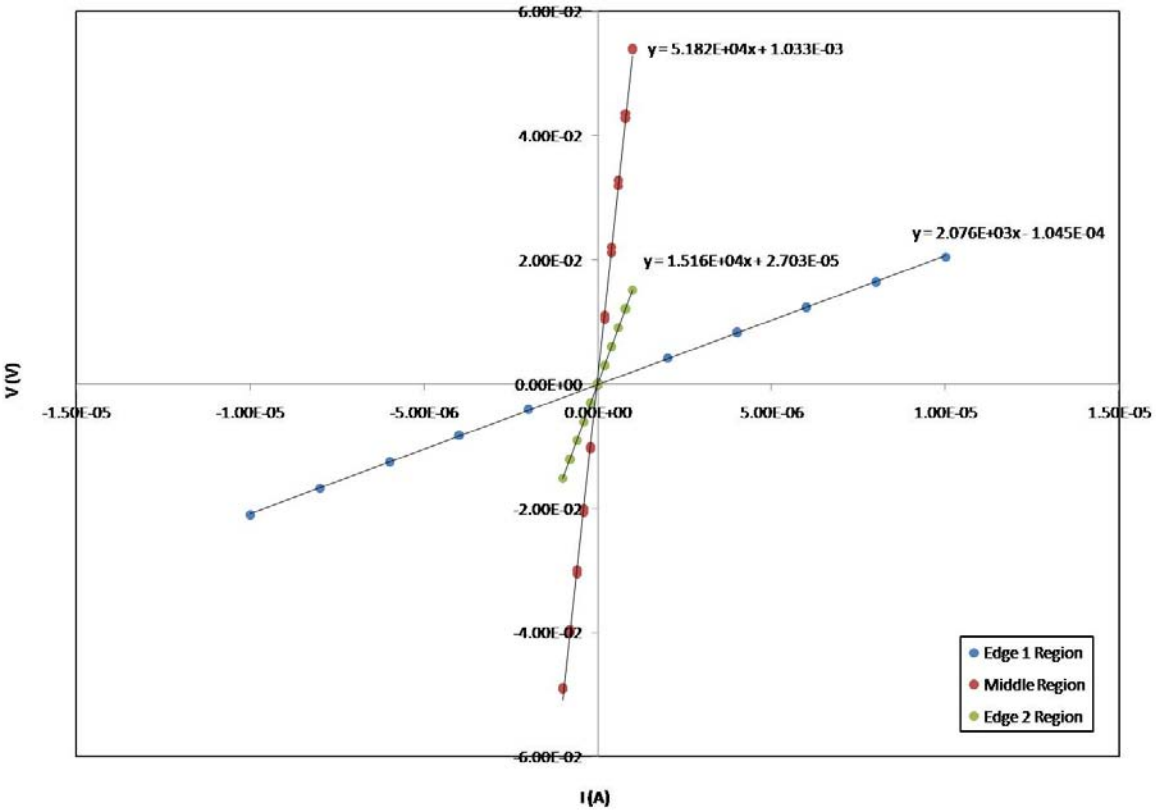

Figure 21: Room temperature IV characterization of 2-coat wafer (slope = resistance).

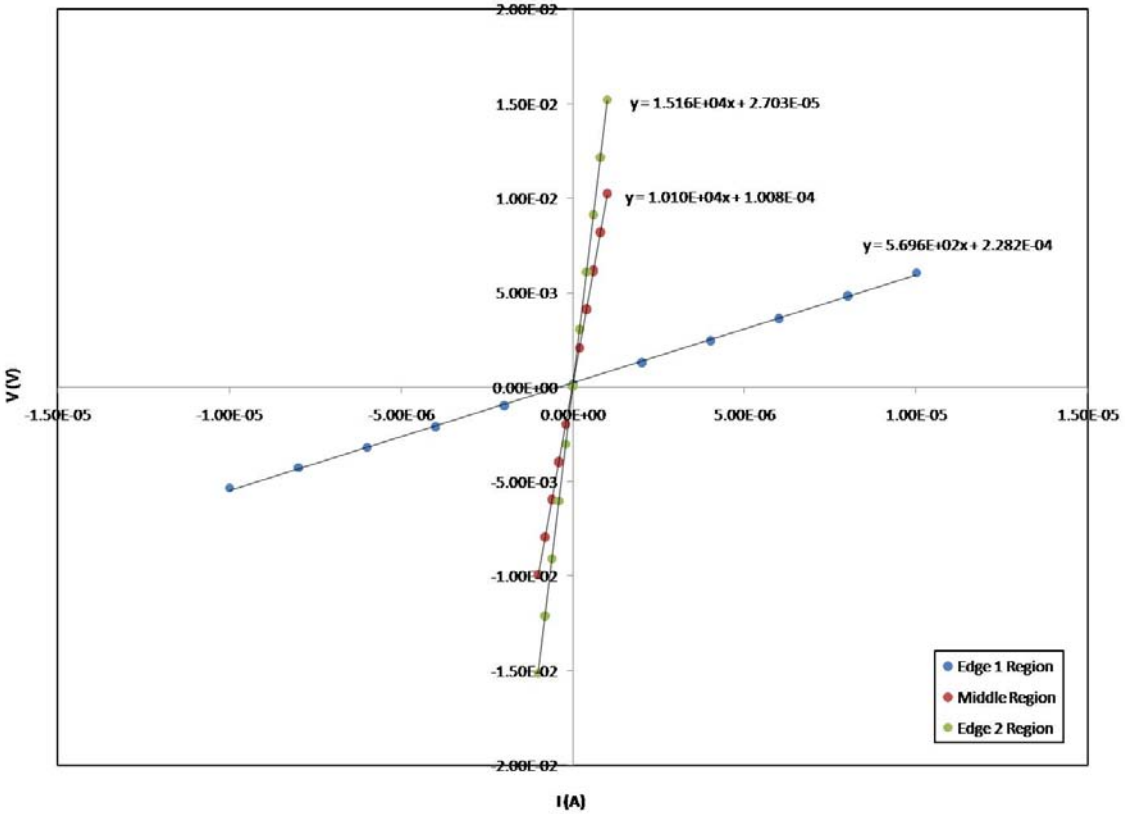

Figure 22: Room temperature IV characterization of 5-coat wafer (slope = resistance).

Table 3 shows the electrical values for both the 2 and 5 coat wafers; the extrapolated resistance (R) values along with the calculated sheet resistance (R_s) and Conductance (G) values. The resistance was determined from the slope of the linear fit of the IV curve for each sample measured. The sheet resistance was then calculated using the following equation:

(1) $Rs = R\ W/L\ (\Omega/\square)$ where, L = 2.00 mm & W = 12.00 mm

And the conductance (G) is calculated using the following equation:

(2) $G = 1/R\ (\Omega^{-1})$

It can be seen from the table that the order of magnitude for the most part is primarily in the $10^4\ \Omega$ range for both the 2-coat and 5-coat samples. This was the basis for the next step which was to conduct a temperature dependent resistance characterization.

Coat	Region	R (Ω)	R (Ω/□)	G (Ω^{-1})
2	Edge 1	2.076E+03	1.246E+04	4.817E-04
2	Middle	5.182E+04	3.109E+05	1.930E-05
2	Edge 2	1.516E+04	9.096E+04	6.596E-05
5	Edge 1	5.696E+02	3.418E+03	1.756E-03
5	Middle	1.010E+04	6.060E+04	9.901E-05
5	Edge 2	1.516E+04	9.096E+04	6.596E-05

Table 3: Resistance, Sheet Resistance and Conductance values for the two (2 coat & 5 coat) wafers for the three respective regions.

The temperature dependent resistance characterization was conducted on the two middle region samples of both the 2-coat and 5-coat wafers. This study was conducted to first verify that the SWNT material coated onto the wafers is dominated by semiconducting SWNTs versus metallic SWNTs. This will be another check to make comparisons between the Pre-DEP and Post-DEP SWNT material. Figure 23 shows a temperature vs resistance curve for the 2-coat and 5 coat samples. It is evident from both curves that the SWNT material at the Pre-DEP stage is mostly semiconducting for both coats.

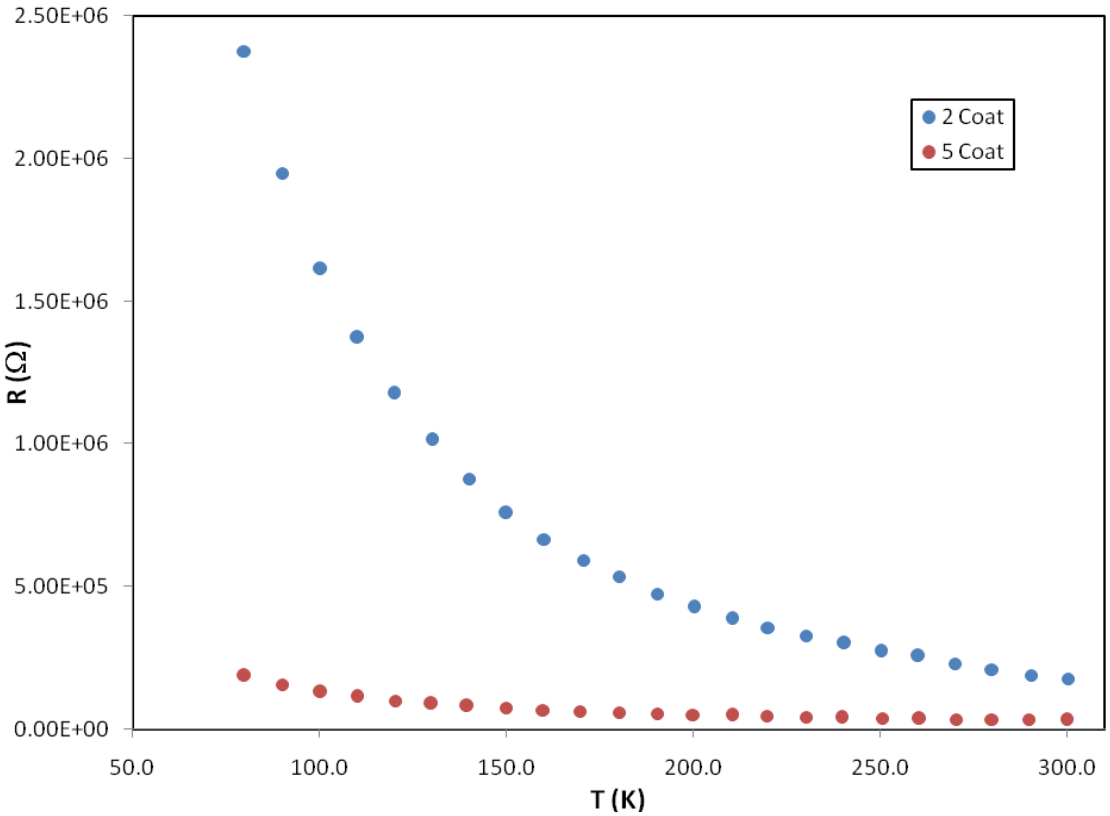

Figure 23: Resistance vs Temperature for the 2-coat & 5-coat (middle region samples).

One of the issues with the spin-coating method is that film coat uniformity is not always consistent. A SonoTek Ultrasonic Deposition system was purchased to remedy this issue such that fabrics could be sprayed uniformly. The system allowed for two advantages over the spin coating method of deposition. This first advantage was that it would produce a more uniform film over a given area. The second advantage is less material consumption over spin coating since the spray coated material could be done on smaller substrates and only on the area of interest. Figure 24 below shows an AFM image of a fabric that was spray coated using the ultrasonic deposition system. Note the consistency of the fabric film which can be controlled and produced without voids. This is important in making the electrical measurements of the systems once comparisons are being made to characterize the Pre-DEP and Post-DEP SWNT material.

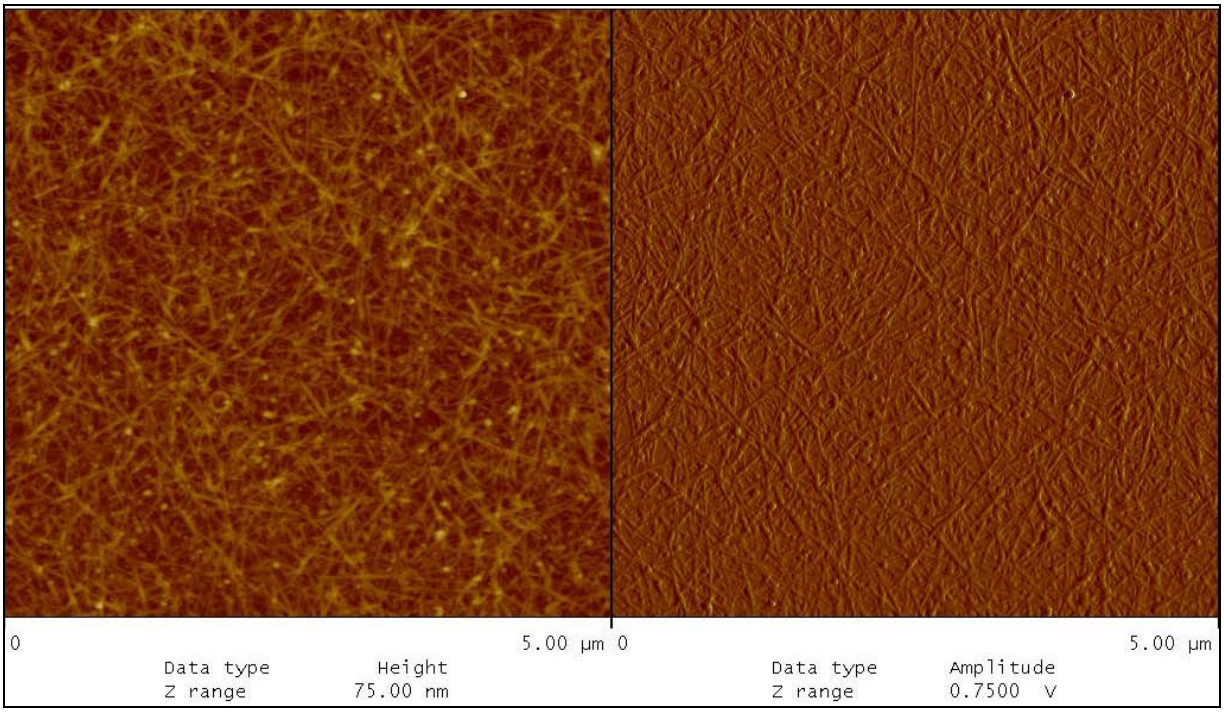

Figure 24: AFM image of SWNT material spray coated onto a glass substrate using the SonoTek Ultrasonic Spray Coating System.

1.3.4.2 Design and Developmental Work of CNT-TFTs

Developing proof-of-concept devices was the next step in demonstrating the applications of type-separated material. One such device is a carbon nanotube thin film transistor (CNT-TFT), which could be fabricated using standard microlithography techniques. Figure 25 below shows a representative schematic diagram of the CNT-TFT device that was under development. The proof-of-concept device was to allow for characterizing/comparing of the Pre-DEP and Post-DEP SWNT material in a device form.

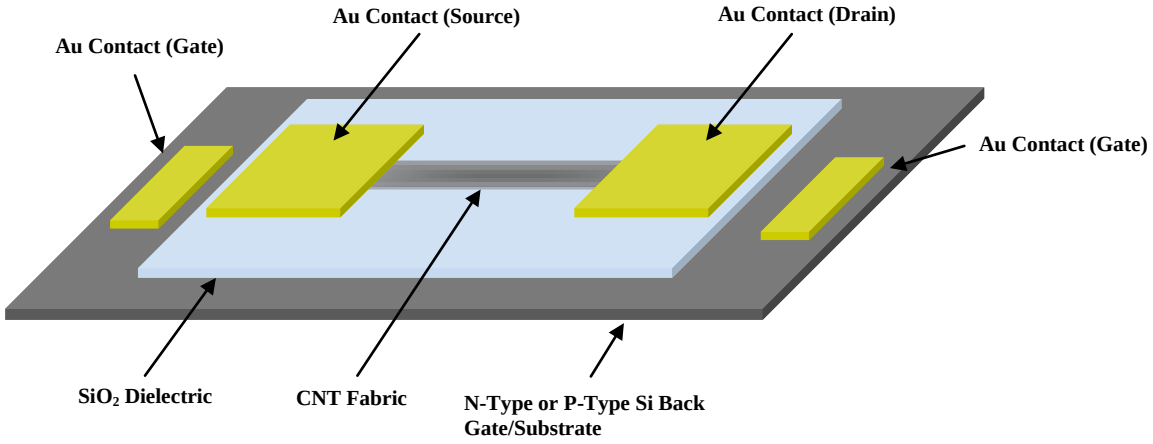

Figure 25: Schematic Diagram of Proposed CNT-TFT Device.

The SEM image in figure 26a shows the source and drain electrode scheme with varying dimensional separation which is where the CNT fabric under test would be patterned. The Au contacts are 125 μm square with a minimum separation of 15 μm up to 100 μm between adjacent contacts. Figure 26b shows an example of a patterned polymer material which currently serves as a place holder to pattern the SWNT material of interest. The separation locations are designated as numeric rows and alphabetic columns. The separation between contacts along with the designation locations are provided in table 4.

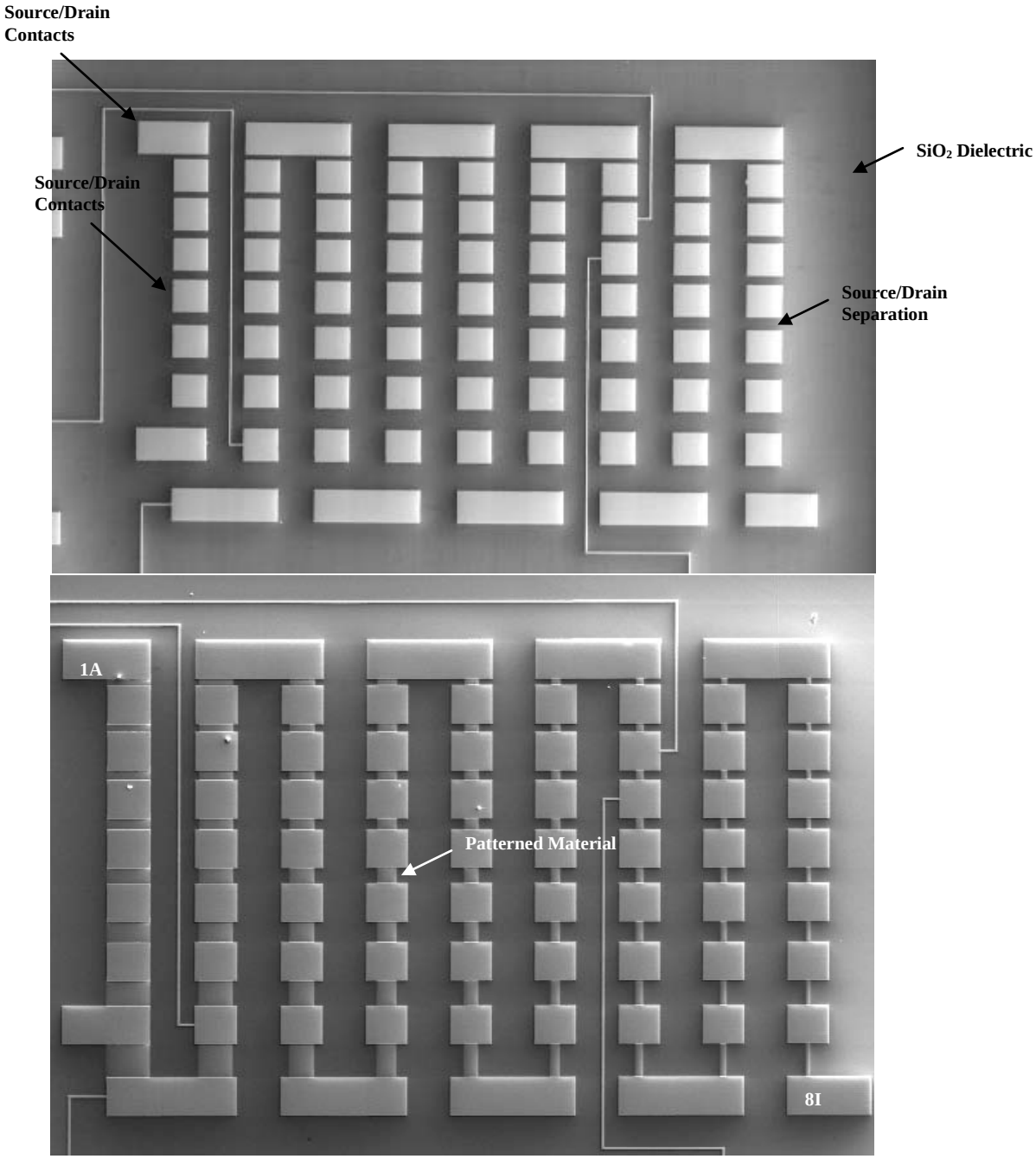

Figure 26: a) SEM image of Source/Drain electrodes configured in an array form with varying separation between Au contacts; b) SEM image showing patterned material where CNT fabric is placed to complete the CNT-TFT device.

	A	B	C	D	E	F	G	H	I
1	15 x 125	15 x 100	15 x 75	15 x 60	15 x 45	15 x 30	15 x 25	15 x 20	15 x 15
2	20 x 125	20 x 100	20 x 75	20 x 60	20 x 45	20 x 30	20 x 25	20 x 20	20 x 15
3	25 x 125	25 x 100	25 x 75	25 x 60	25 x 45	25 x 30	25 x 25	25 x 20	25 x 15
4	30 x 125	30 x 100	30 x 75	30 x 60	30 x 45	30 x 30	30 x 25	30 x 20	30 x 15
5	45 x 125	45 x 100	45 x 75	45 x 60	45 x 45	45 x 30	45 x 25	45 x 20	45 x 15
6	60 x 125	60 x 100	60 x 75	60 x 60	60 x 45	60 x 30	60 x 25	60 x 20	60 x 15
7	75 x 125	75 x 100	75 x 75	75 x 60	75 x 45	75 x 30	75 x 25	75 x 20	75 x 15
8	100 x 125	100 x 100	100 x 75	100 x 60	100 x 45	100 x 30	100 x 25	100 x 20	100 x 15

Table 4: Dimensional (row height x column width) designation. All dimensions are in microns.

In light of characterizing these CNT-TFT devices as well as conducting the basic room temperature IV and temperature dependent resistance measurements, a Keithley 4200 semiconductor characterization system (SCS) was purchased. This system would also allow us to obtain parametric data of the CNT-TFTs once they were developed. The system was chosen for these specific measurements because it conforms to and supports the new IEEE Standard P 1650™-2005: IEEE Standard Test Methods for Measurement of Electrical Properties of Carbon Nanotubes. Initial work with this system included set up, which included interfacing with an existing 4-wire probe station, an existing temperature variable cryostat and familiarization with the systems GUI.

During the course of development of the CNT patterned fabrics it was determined that some of the etching steps during the lithography processes actually affected the electrical properties of the SWNT fabric. There was some difficulty in getting the CNT fabrics patterned. This was a critical step that we unfortunately were not able to overcome in terms of the SWNT fabric's electrical properties consistency after the lithography patterning process.

1.3.4.3 Modification of Project Tasks

The 5th quarter's work for this project involved the restructuring of project tasks. The original project tasks were divided among the three groups working in collaboration on this project; Unidym, Inc (buckytube material provider), Brewer Science, Inc (buckytube purification and type separation developer), and JVIC-MSU (buckytube application and characterization). During the 4th quarter of this project, Unidym went through an internal restructuring and closed its materials development division. In light of this restructuring other commercial buckytube material vendors had to be investigated.

At this point BSI had completed its task to develop a dielectrophoresis process to separate the SWNTs after their established purification process which produces stable surfactant-free purified SWNT dispersions. However, the process still required refinement and scale-up to produce large volumes of material. At this point JVIC continued the work independently to refine the process to allow for scale up and test the materials using standard characterization techniques as well as testing of application test devices.

1.3.4.4 Alternative Buckytube Supply Vendors

With Unidym going through a corporate restructuring which involved the closure of its buckytube materials division, other buckytube supply vendors had to be investigated. A number vendors were investigated which included Southwest Nanotechnologies, Inc, Swan Chemcial, Inc, and Nanolab, Inc. The initial work involved an investigation of each of the company's material data sheets to determine the purity levels as well as chirality information of their as-produced SWNT material. Out the various companies that were investigated, three were determined to provide the highest quality material. The three vendors that were chosen for their materials evaluation included Southwest Nanotechnologies, Inc, Swan Chemcial, Inc, and Nanolabs, Inc.

1.3.4.4.1 Qualification of Buckytube Supply Vendors

Raman spectroscopy was performed on the different SWNT materials that were purchased for comparison of quality and diameter distribution of tubes comprising the materials. These materials include Southwest Nanotechnologies SWeNT CG100, SWeNT CG200X, NanoLabs D1.5L-1-5-S CVD, and Thomas Swan PR0925. These materials were compared to the Unidym HiPCO material to determine which vendor's materials most closely compared for ease of dispersibilty, diameter distribution and quality/purity (figure 27). Conditions for the sample preparation are as follows; 10 grams of SWNT material was placed in 100 ml of 0.5% wt. sodium dodecyl benzene sulfonate (SDBS) solution, the solution was then horn sonicated for 30 minutes at 72% amplitude using a ½" probe. 10 ml of solution was used to prepare a vacuum filtration disc. Raman was then performed on the filter disc using lasers of 532 nm (2.33 eV), 633 nm (1.96 eV), and 785 nm (1.59 eV) wavelengths.

The D band known as the defect band gives insight as to the amount of defects in the sample, a higher intensity is indicative of more defects. The degree of broadness in the peaks indicates either defects in the SWNTs for narrower peaks or the level of amorphous carbon present for broader peaks. From the shape of the D mode of the SWNT samples measured, it would seem that there is more amorphous carbon present than tube defects. The quality or purity of the sample is determined by the D/G ratio of the Raman spectra, which is shown in table 5 below. It is apparent that the SWeNT CG200X has the highest quality of tubes with a D/G ratio of 0.024, while the NanoLabs D1.5L-1-5-S has the lowest quality with a D/G ratio of 0.050. The purity for the NanoLabs and HiPCO materials closely matches that of their data sheets with a purity >95% and ~97% purity, respectively.

Sample	D	G	D/G
SWeNT CG100	41428.3	1247750	0.033
SWeNT CG200x	41435.2	1755750	0.024
NanoLabs D1.5L-1-5-S	105598	2101880	0.050
Thomas Swan PR0925	106320	2197210	0.048
Unidym HiPCO	75637.5	1923760	0.039

Table 5: D/G Ratios for the various materials tested.

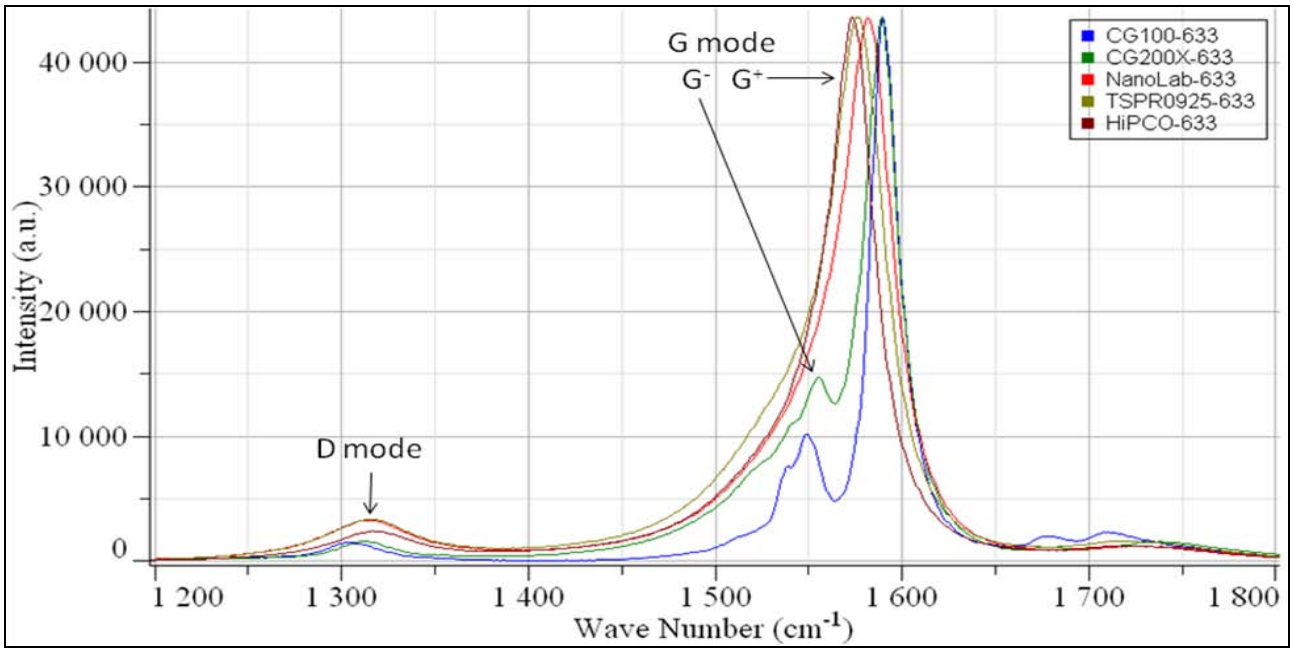

Figure 27: Raman of the D mode and G mode using 633 nm laser.

The shape of the G mode gives insight into whether the species of SWNTs are semiconducting or metallic. The presence of the G^- peak of the G mode suggests that the SWeNT materials, CG100 and CG200X, both contain amounts of metallic SWNTS (m-SWNTs). The other samples' lack of a G^- peak suggests overwhelming semiconducting SWNT (s-SWNT) populations. The radial breathing mode (RBM), between 100 cm^{-1} and 400 cm^{-1}, gives the tube populations diameter distribution, electronic properties and aggregation states. Another feature of note is the existence of a bundling peak in the RBM due the effects of overlapping energies of tubes.

The diameter distribution of the samples studied was between 0.6 nm to 1.7 nm, with the NanoLabs material having the largest distribution of 0.6 nm to 1.7 nm and both SWeNT CG100 and CG200X having the smallest distribution of 0.6 nm to 1.3 nm. The Thomas Swan materials compared similarly to the Unidym HiPCO material with both having a diameter distribution of 0.7 nm to 1.7 nm. It was determined that the SWeNT CG200X material seemed to be better in quality than the other materials that were investigated, and best compared to the HiPCO material.

Sonication conditions were studied once it was determined that the SWeNT CG200X was the material of choice to determine the best conditions for dispersion with the least amount of tube destruction. Both an amplitude and time study were conducted for this purpose. The graphs in figure 28 below show the Raman results of this study, where it was determined that a 50% amplitude for a 30 minute sonication period had the least amount of tube destruction.

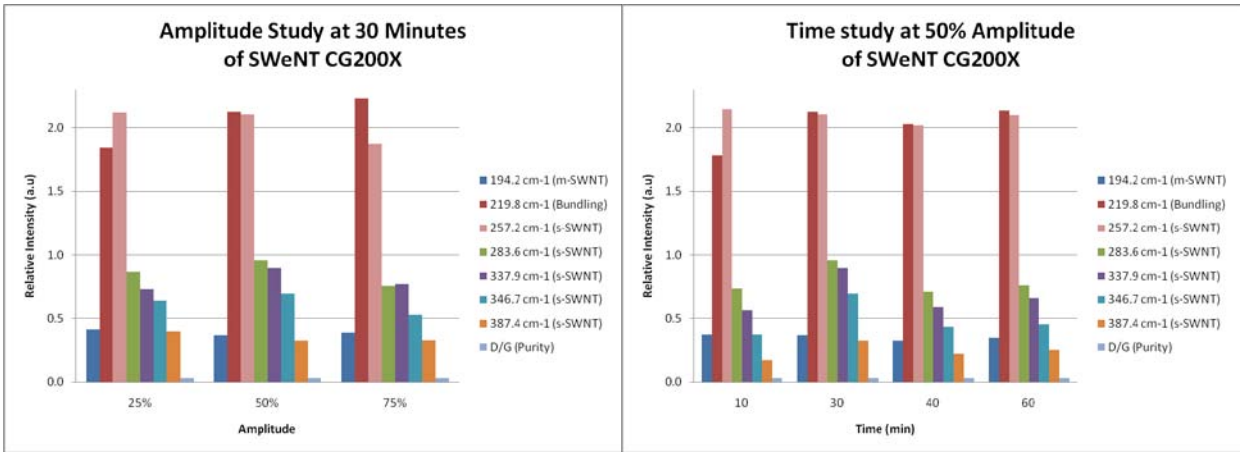

Figure 18: Sonication amplitude and time showing relative amounts of tubes in solution for SWeNT CG200X.

The sonication time solutions were then centrifuged to see how well the SWNTs dispersed in the solution. Absorbance was measured for the pre and post centrifuged solutions to see a change in material removed from the solution. From figure 29, it shows that the 60 minute sonication sample had a higher concentration of SWNTs remaining in the solution because of the small amount of change in absorbance. This would indicate that a 60 minute sonication time will yield the best dispersion, however the Raman data suggests that the 30 minute sonication time had the least amount of tube destruction. Even if there is more material in solution after a 60 minute sonication, the tubes would have more defects. Therefore the best sonication conditions for the SWeNT CG200X will be at 50% amplitude for 30 minute sonication time.

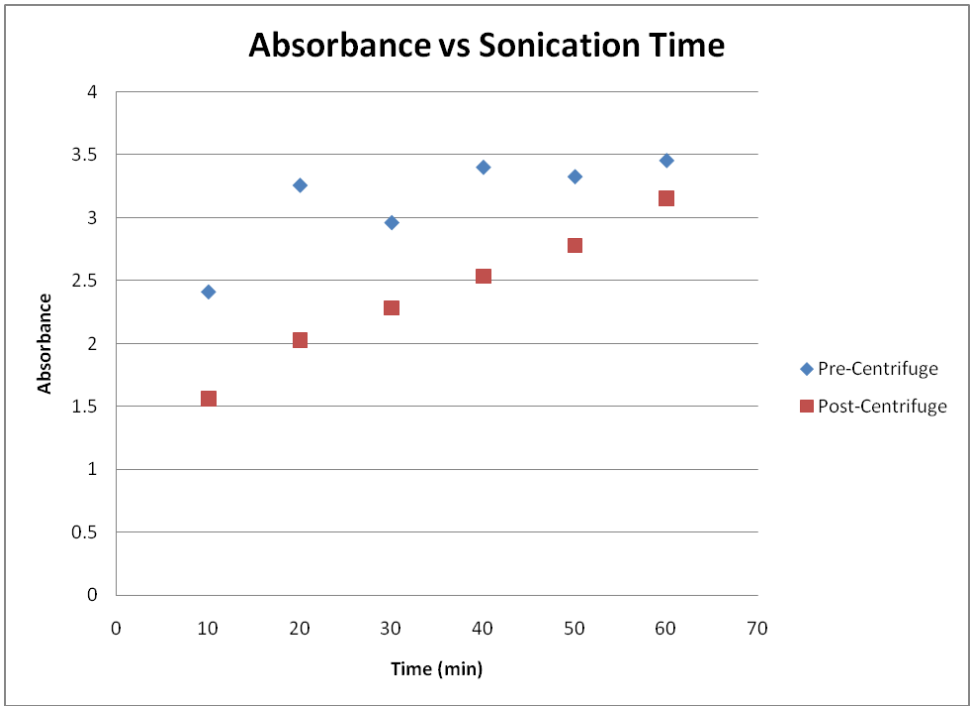

Figure 29: Absorbance of pre and post centrifuge solutions with different sonication times.

1.3.4.5 Continuous-Flow Type-Separation System

Work into refining the setup for a continuous flow system was continued where it was shown that refining the electrode geometry yielded better results as shown in figure 30, which shows both an AFM and SEM image of the m-SWNTs that have aligned between the electrodes due to dielectrophoresis.

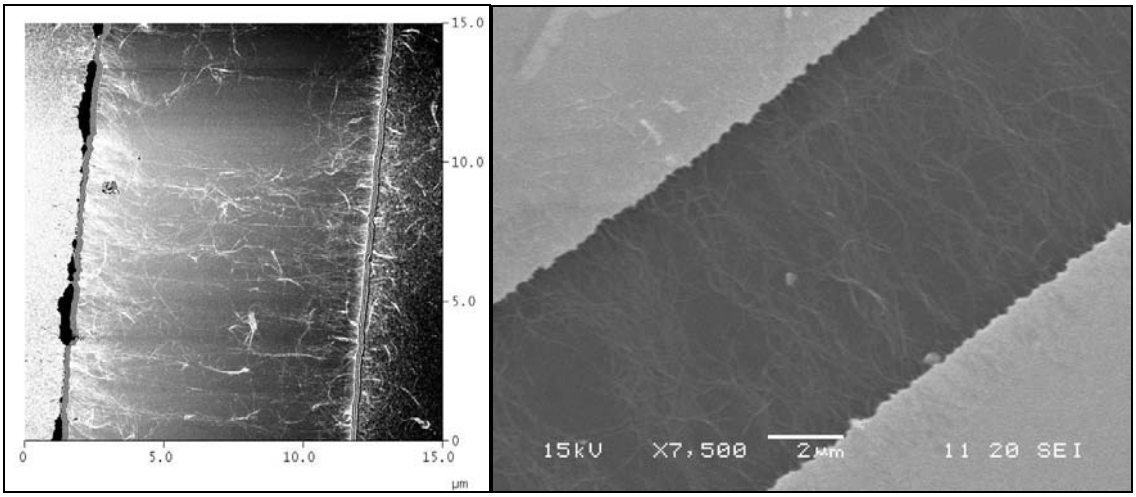

Figure 30: AFM (left) and SEM (right) images of m-SWNTs aligned between electrodes.

A continuous flow dielectrophoresis system was designed to accommodate a number of different electrode geometries onto a fluidic chamber system that would allow for greater separation. This would be done by creating a multiple electrode scheme that is connected in a parallel configuration similar to capacitors in parallel. Each electrode system (1cm x 1cm) chip can then be housed in a fluidic chamber with chambers that run in series but the electrodes being electrically connected in parallel. This would allow for a single AC signal source to provide the same amplitude over multiple electrodes simultaneously. The setup design is illustrated in figure 31 below.

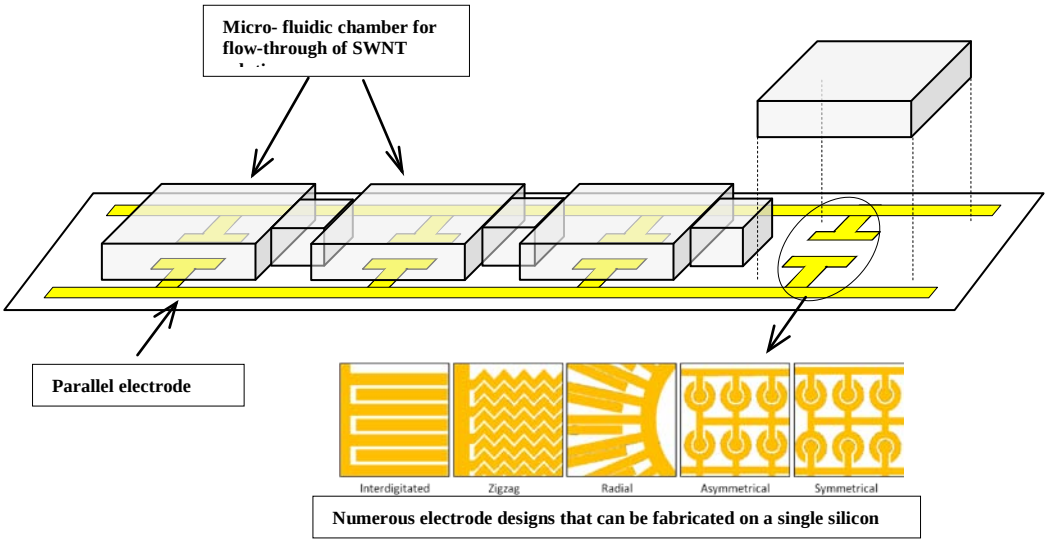

Figure 31: Continuous-Flow electrode setup for scale up of dielectrophoresis process.

1.3.4.5.1 Dielectrophoresis Electrode Design

The parallel electrode geometry that was designed would allow for more surface area for SWNT type-separation. It was also determined that out of all the electrode geometry patterns two designs; radial and inter-digitated yielded the highest separation of metallic SWNTs from solution. The micro-electrode design is shown in figure 32 below, where there are 8 electrode cells per configuration and one being radial and the other being inter-digitated.

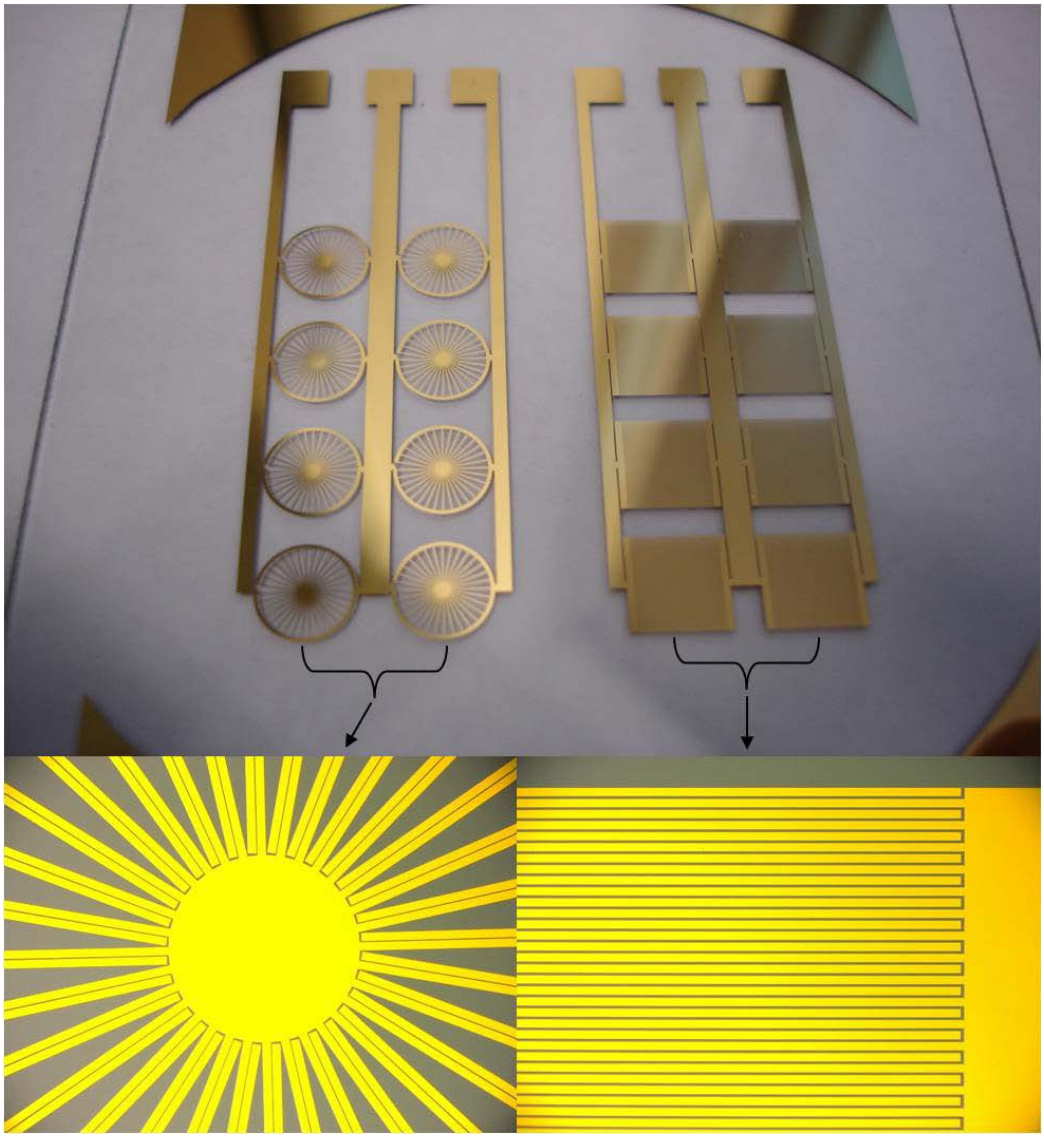

Figure 32: Top image is a full patterned electrode design with radial on the left and inter-digitated on the right with a zoomed optical microscope close-up of each electrodes configuration below.

These electrode schemes were dimensionally designed such that they could be house in an off-the-shelf fluidic cell chamber system. The fluidic cell chamber system was modified such that it would allow for a continuous flow rather than a static chamber for each cell. Figure 33 below shows an image of the continuous flow setup that was developed. The manipulator probes applied the AC signal to the electrodes along with measurement of the signal.

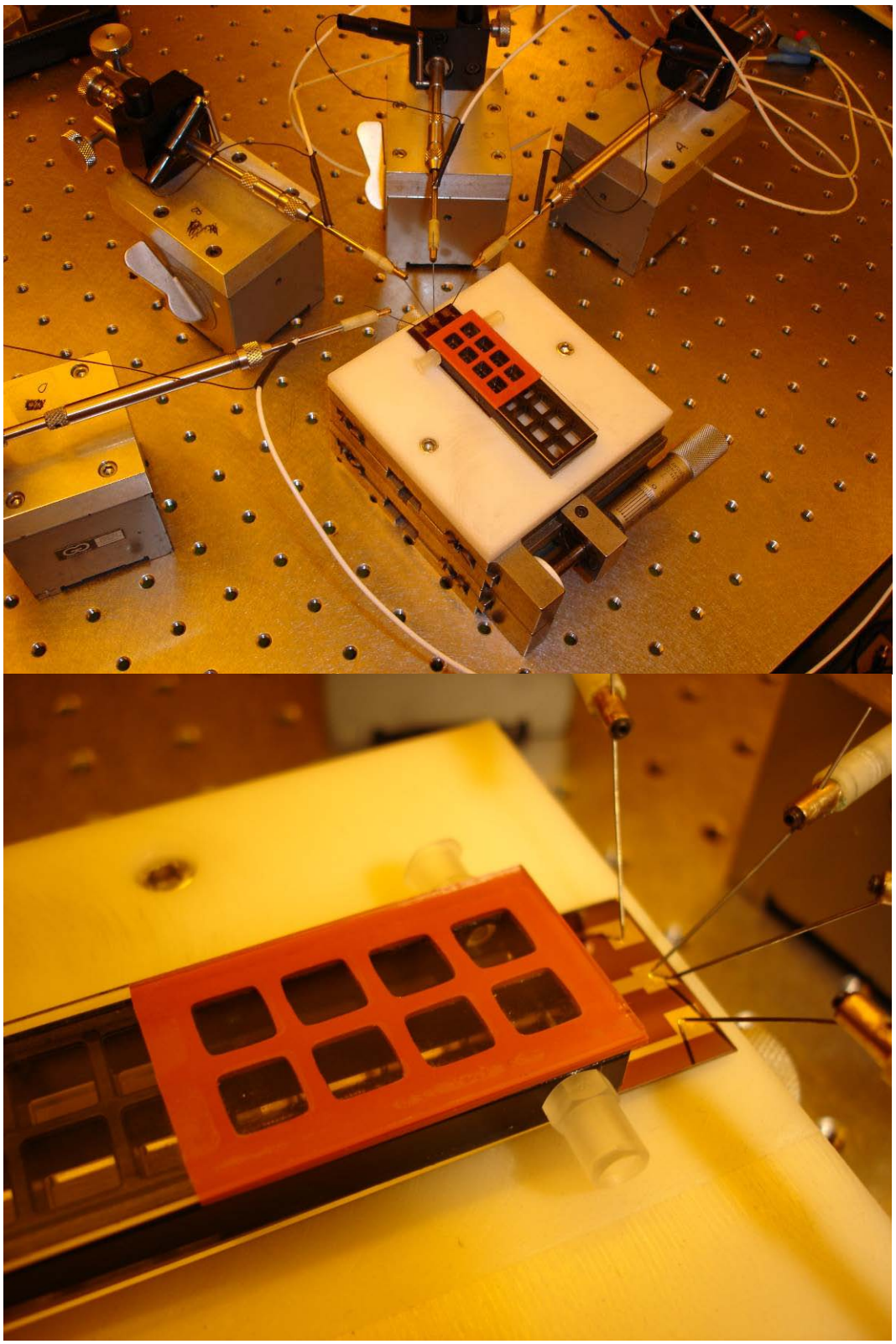

Figure 33: Top image is the continuous flow dielectrophoresis system setup and bottom image is a close-up of the system fluidic chamber system.

The system mode of operation is illustrated below in the figure 34. The solution is fed into the inlet using either a syringe pump or a peristaltic pump at rates of microliters or nanoliters per hour. As the AC signal is applied to the electrodes, the solution that runs through each well chamber in a continuous or re-circulating fashion is processed for type separation to create a semiconducting rich solution where the metallic SWNTs are immobilized onto the metal electrodes. This setup produces milliliters of volume and still requires further refinement to scale up to produce liter level volumes of material.

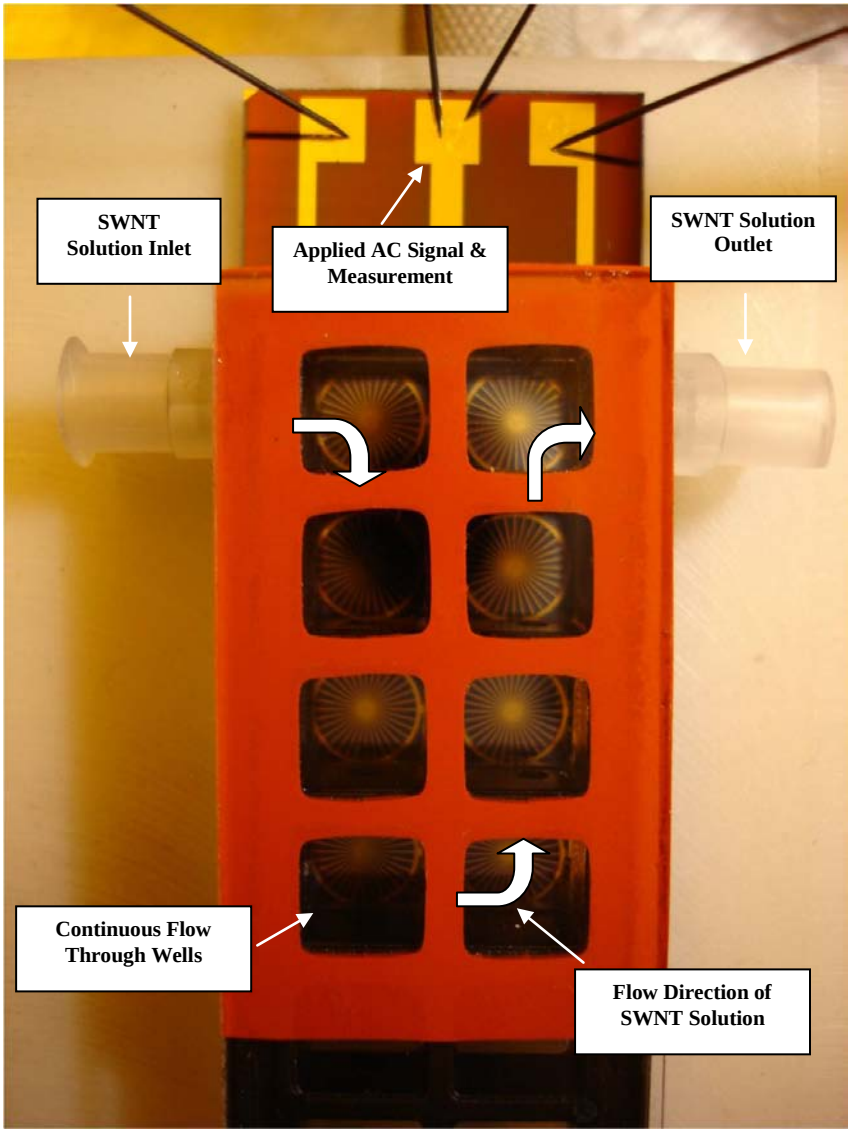

Figure 34: Top-view image of system design and flow scheme mode of operation.

The system showed significant improvement over previous design systems where a large amount of metallic SWNTs were evident on the electrodes as shown in figure 35. As can be seen with in this case the radial configuration shows a large amount of metallic SWNT alignment between the metal electrodes. This level of separation was also observed with the inter-digitated electrode geometry. Figure 36 shows an SEM image of the m-SWNTs having aligned between the Au electrodes.

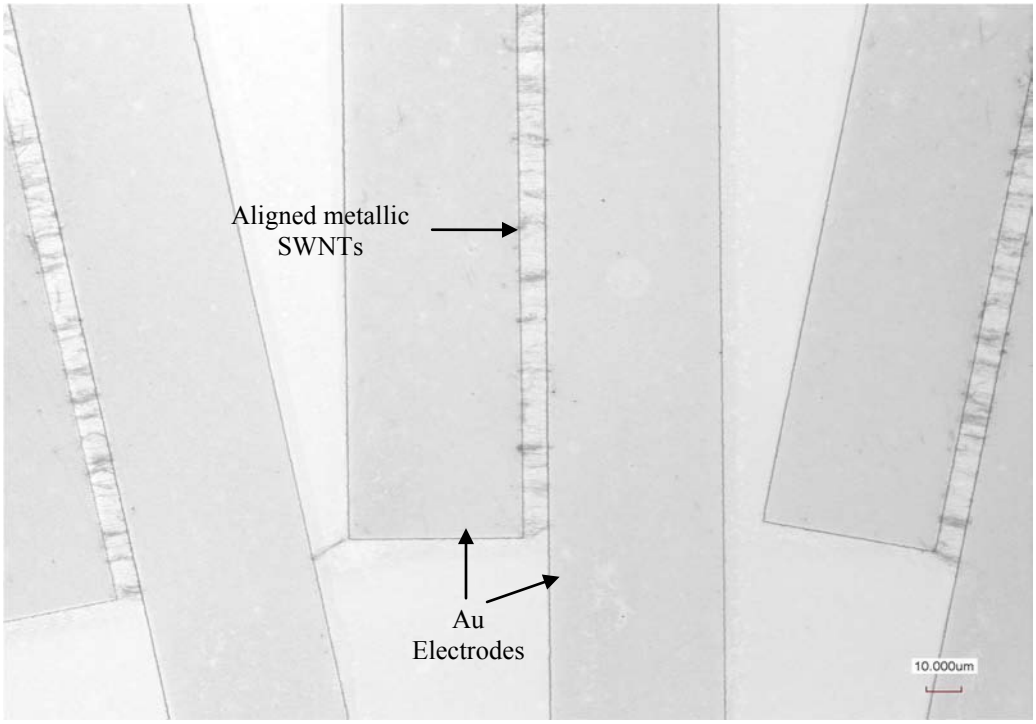

Figure 35: Confocal Laser Scanning image of Post-DEP where metallic SWNTs are aligned between the Au electrodes of a radial geometry configuration.

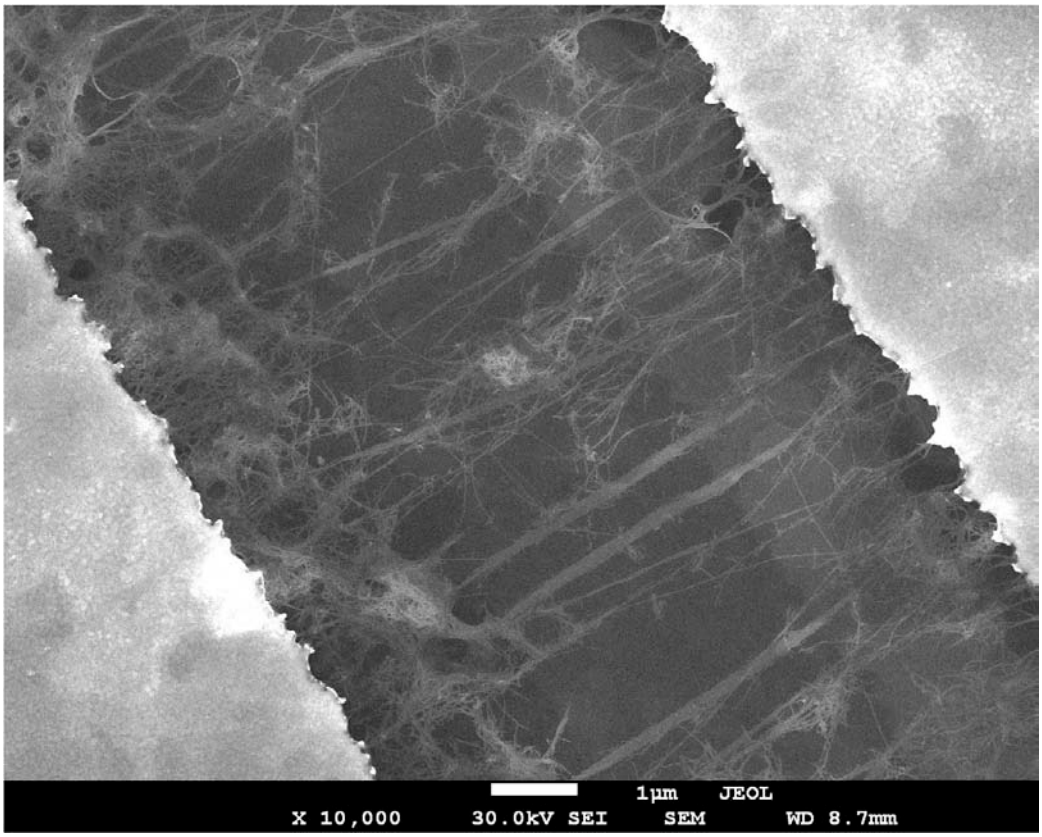

Figure 36: Scanning Electron Microscope image of Post-DEP with metallic-SWNTs aligned between the Au electrodes.

To make the system more efficient the electrodes were easily cleaned using a Plasma Etching process such that they could be re-claimed and used again. The continuous flow system was designed such that the electrode could be cut to size and be inter-changed with the fluidic well chamber system such that the multiple electrodes could be fabricated and used one after the other. To increase the volume of production, a higher number of electrode cells on a single setup needs to be designed such that a larger area is available for type-separation and scale up.

Electrical characterization was conducted on the Pre-DEP solution and the Post-DEP solution to conduct a quick check to determine the degree of type-separation using electrical test methods. It was determined that the quickest check would be to conduct a temperature dependent resistance measurement to see the ΔR/R change as a function of decreasing temperature down to cryogenic temperatures. Figure 107 shows that data plotted of a batch of Southwest Nanotechnologies CG200x material that was characterized both Pre and Post-DEP. As can be seen the ΔR/R change is higher for the Post-DEP material versus the Pre-DEP material with change of 29.41%. This indicates that the quantity of semiconducting SWNTs in the batch of material run through the continuous flow dielectrophoresis setup was higher than compared to before it was run through the system. Further studies are still required to optimize this separation method in increase overall separation yield percentage per run.

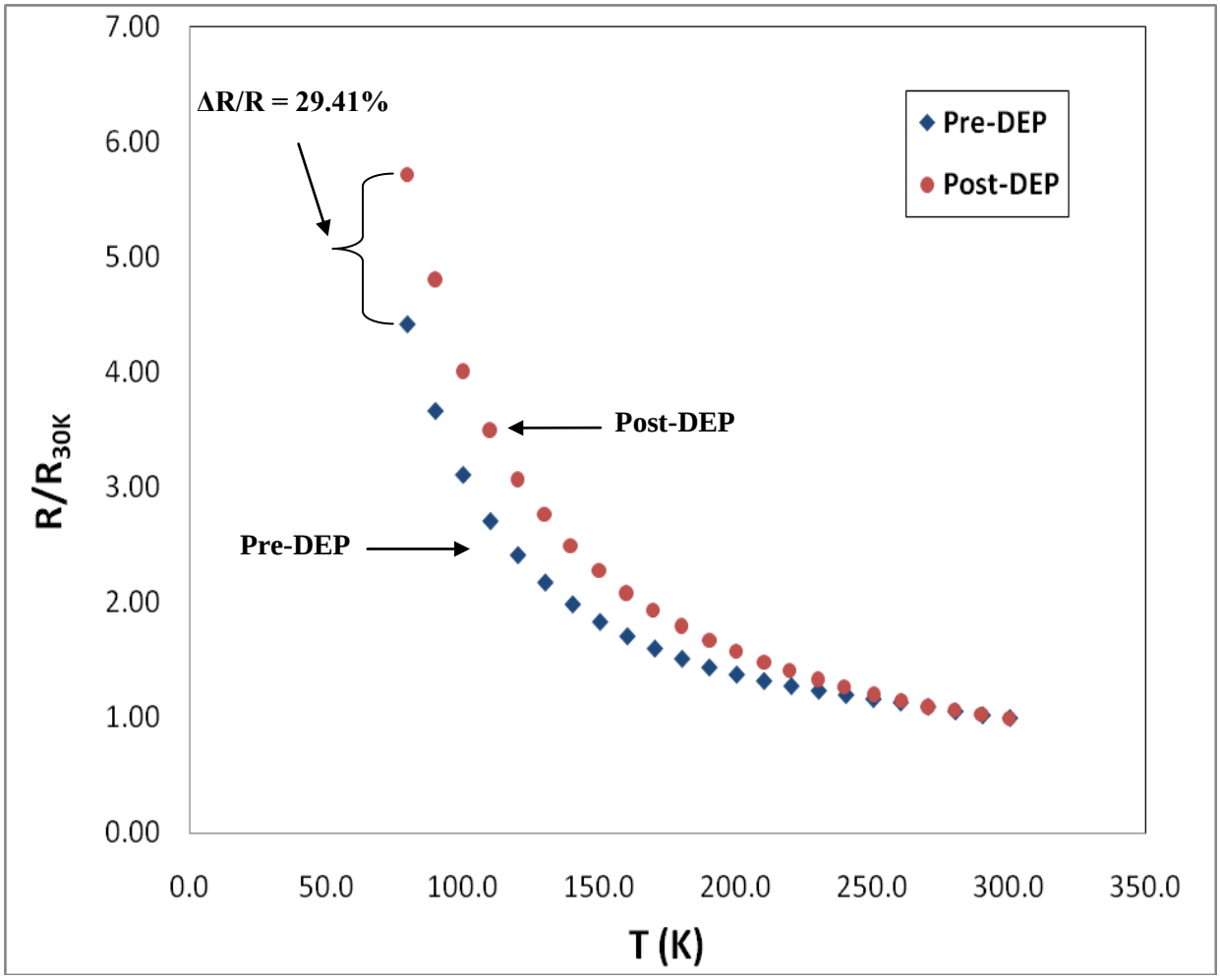

Figure 107. Resistance vs Temperature curve normalized to R @ 300K for each sample run to compare resistance change between Pre-DEP and Post-DEP

1.4 Conclusion

In conclusion, it has been demonstrated that a supply of SWNT material can be separated based on electronic-type via the dielectrophoresis method. A bench scale dielectrophoresis system has yielded milliliter amounts of type-separated material, specifically semiconductor enriched SWNTs. At this point the levels of enrichment are still low and need further refinement to meet the levels required for high level integration into next generation electronics. The restructuring of Unidym materials development division required a modification of tasks for the project where the majority of the effort was focused on the dielectrophoresis setup. As most of the effort during the last portion of the project being focused on the dielectrophoresis system, this resulted in the device application portion of this project to not be fully completed.

The base CNT-TFT device platform was designed and implemented with the patterning of the SWNT fabric which remained pending. Out of the 12 batches that were obtained from Unidym only a couple of the batches seemed to work with BSI's purification process. The inconsistency of the raw as-produced material was a limiting factor in BSI's effort to produce a high purity surfactant free stable solution of SWNT material for most of the materials provided. BSI's initial designs for the dielectrophoresis setup were optimized to yield higher separation, but there is still room for improvement and scale-up.

It has been determined that a number of different SWNT manufacturers can be utilized for the type-separation process. One the main concerns, Post-DEP are whether or not the materials can then be purified using BSI's proprietary process. For large volume production, the purification process that is implemented requires the batch of material (Post-DEP) to be consistent from batch to batch. It was determined that the Southwest Nanotechnologies SWeNT CG200X grade of material seemed to most closely resemble the properties of the HiPCO SWNTs. Another alternative would be to purify the SWNT material first and then conduction type-separation. It was noticed that purifying the SWNT material first did not yield separation in some cases compared to SWNT solution being dispersed in surfactant based solution. It is hypothesized that this may be due to the functional groups (COOH) rendering the metallic tubes inert and therefore not adhering to the electrodes during dielectrophoresis; this however needs to be further investigated.